A multi-frequency view of γ-ray selected Blazars

Paolo Giommi
Italian Space Agency, ASI

AGN : Two main categories

1. *Dominated by thermal emission from accretion disk* - TD-AGN (>~90 %)
2. *Dominated by Non-Thermal radiation - jet emission* - NT-AGN (< 10%)

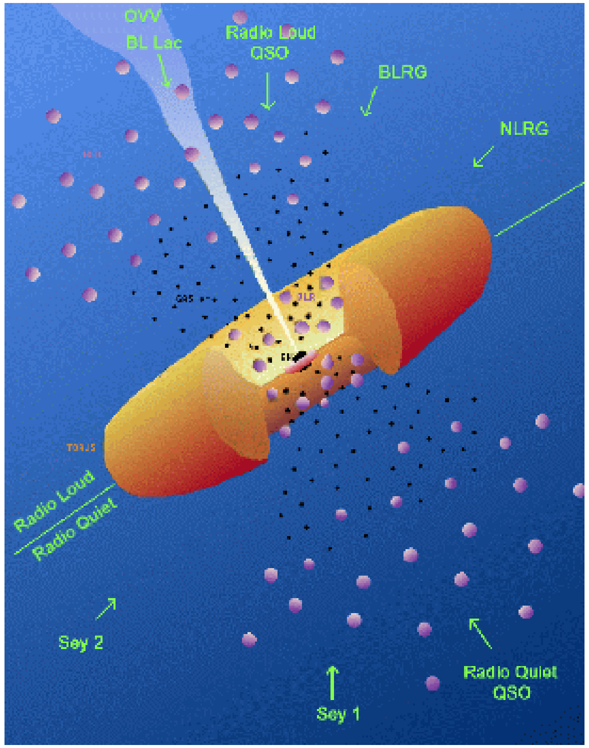

As of today, about 2,800 blazars are known. Only small good statistical samples exist so far, each including a few hundred objects at best! …but Fermi, Planck and other facilities are going to change this soon

Blazar research is much less developed than that of TD-AGN. Still, blazars dominate the extrag. sky in a number of emerging observational windows (μ-wave, hard X-ray, γ-ray, TeV)

The BZCAT blazar list

Massaro et al. 2009, A&A 495, 691

~ 2800 blazars

1577 FSRQs
964 BL Lacs
250 uncertain type

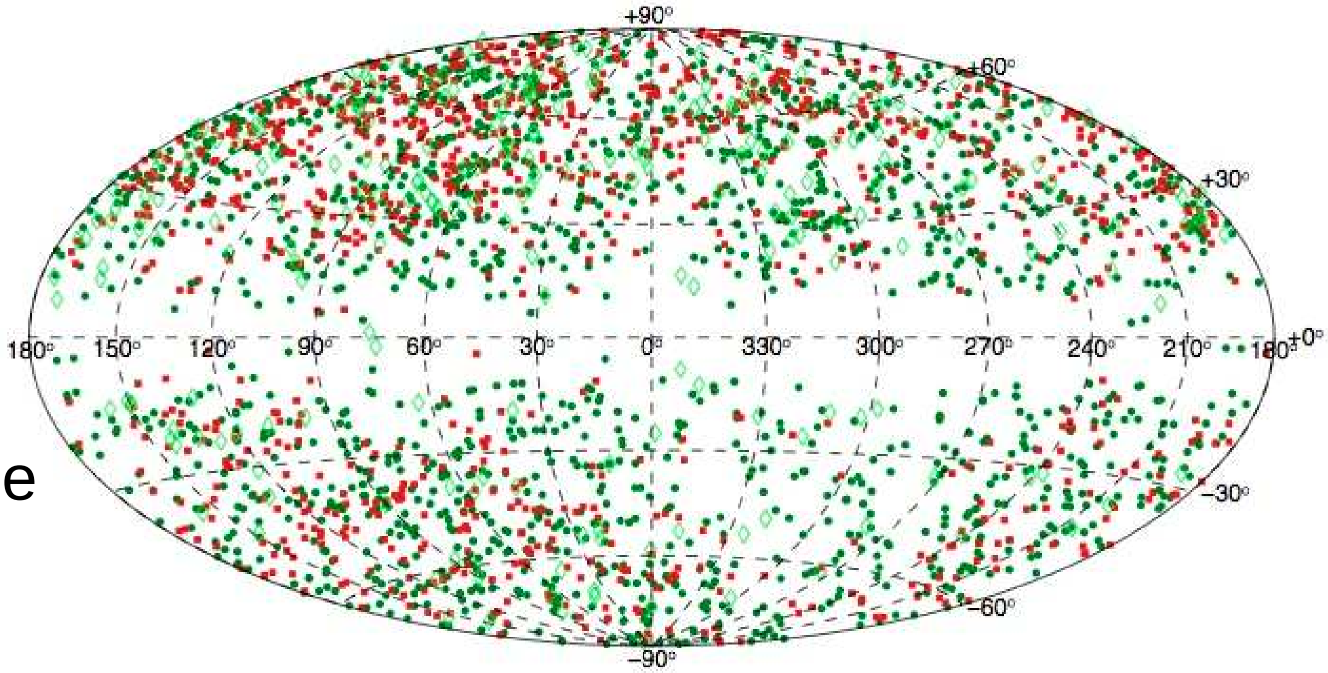

On-line version at ASDC http://www.asdc.asi.it/bzcat

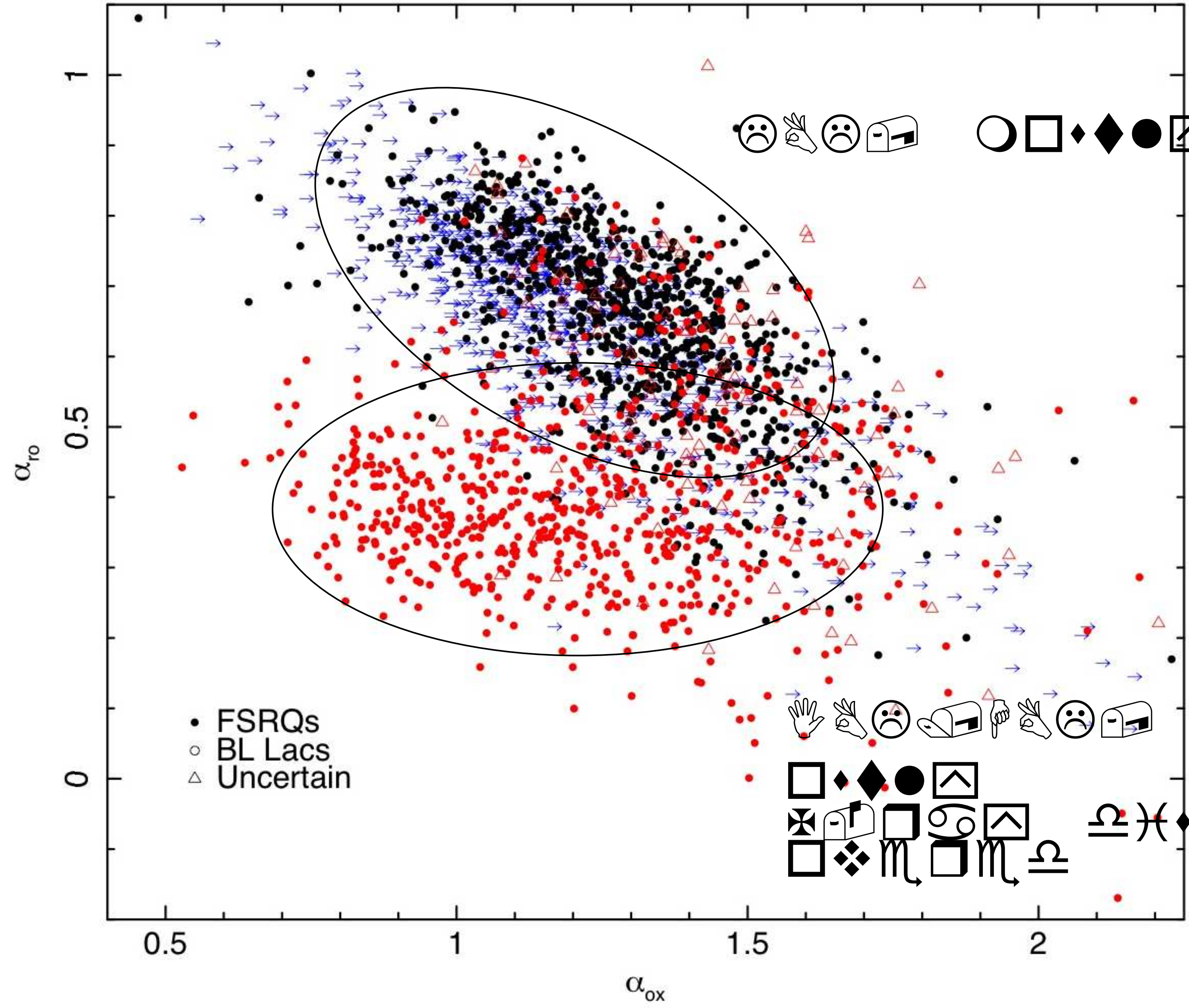

FSRQs
BL Lacs
Uncertain
α_{ro}
α_{ox}
0.5
1
1.5
2
0
0.5
1

The Fermi August-September-October sky

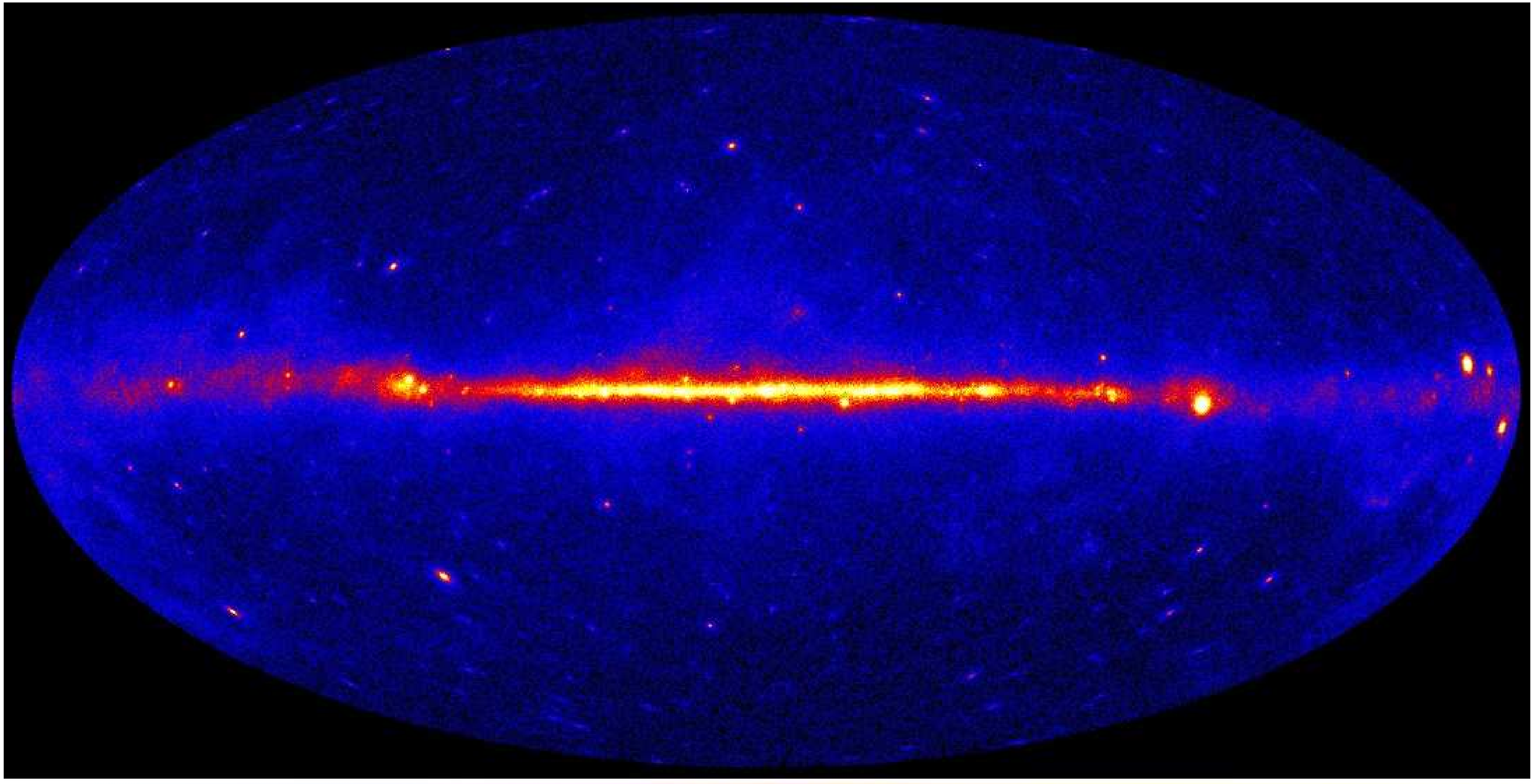

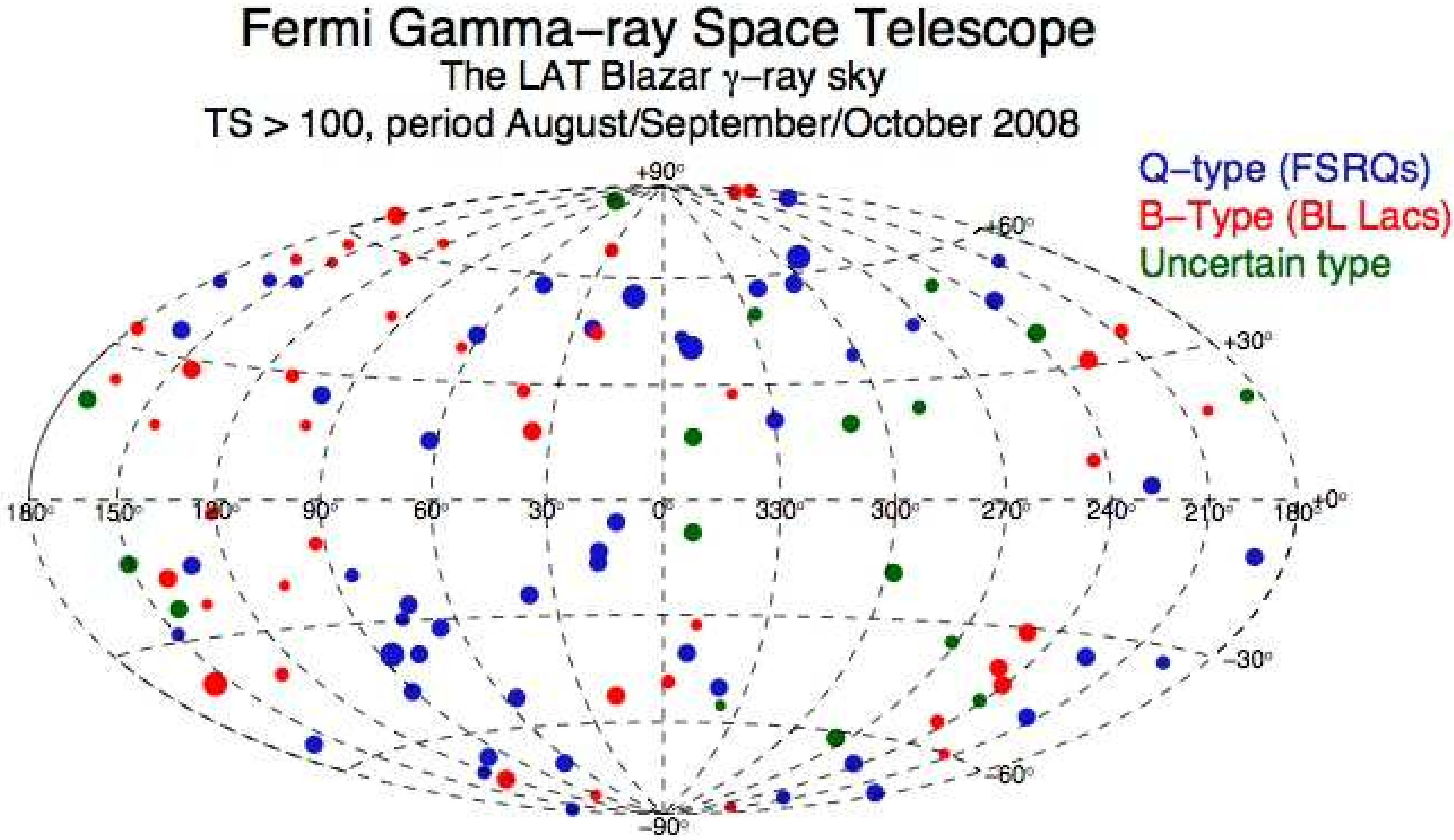

Abdo et al. 2009, ApJ, 700, 597

132 sources at |b| > 10^{o}
At least 106 are blazars

The Fermi LAT Bright AGN Sample (LBAS) Abdo et al. 2009

- 106 bright (significance > 10 σ) AGN at |b| > 10
- 58 FSRQs, 42 BL Lacs, 4 BZUs,

  2 Radio galaxies (larger fraction of BL Lacs than EGRET)
- Only ~30% detected by EGRET (High Variablity)
- Many BL Lacs are of the HBL or IBL type with hard gamma-ray spectrum

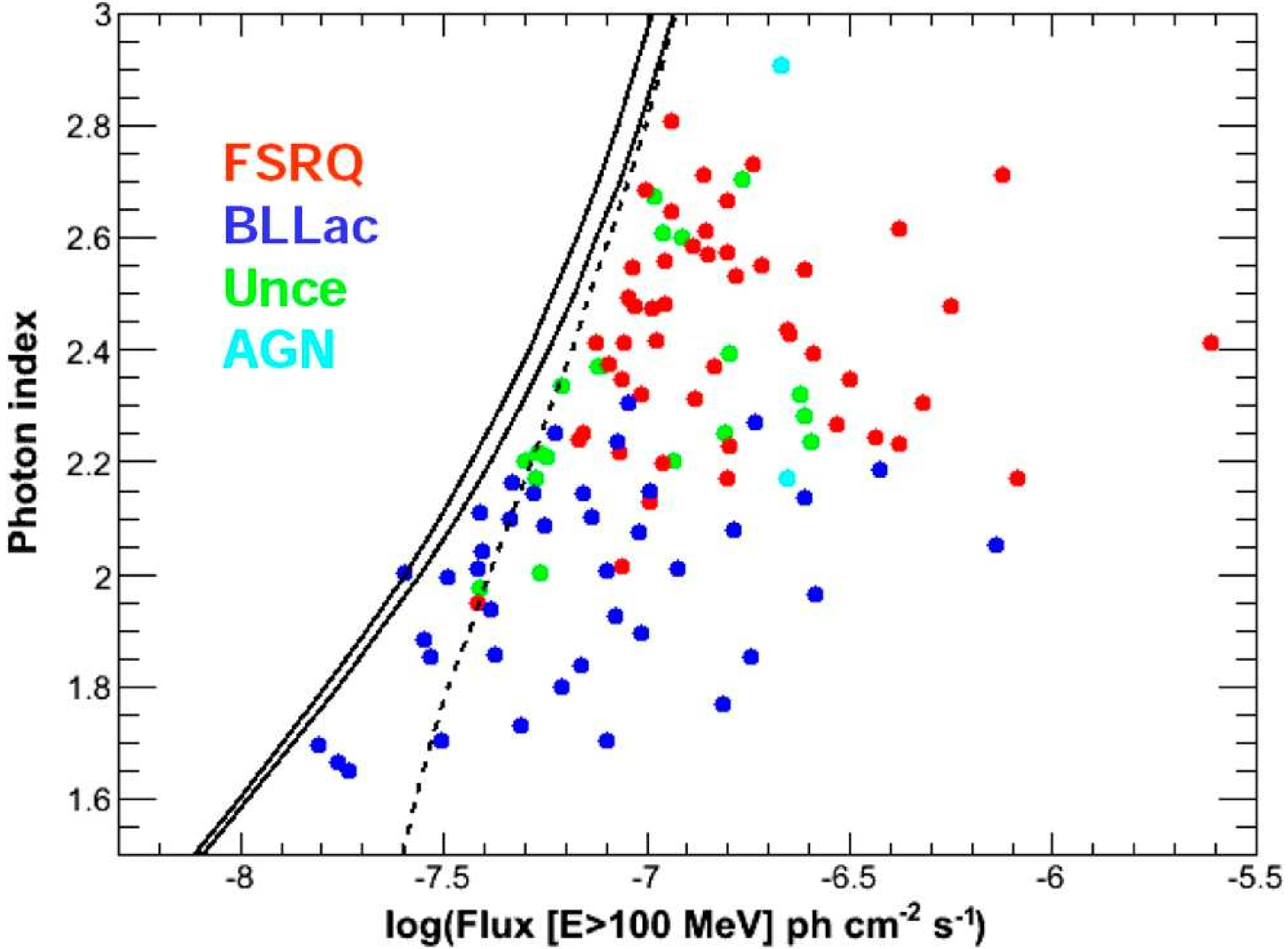
FSRQ
BLLac
Unce
AGN
Photon index
3
2.8
2.6
2.4
2.2
2
1.8
1.6
-8
-7.5
-7
-6.5
-6
-5.5
log(Flux [E>100 MeV] ph cm^{-2} s^{-1})

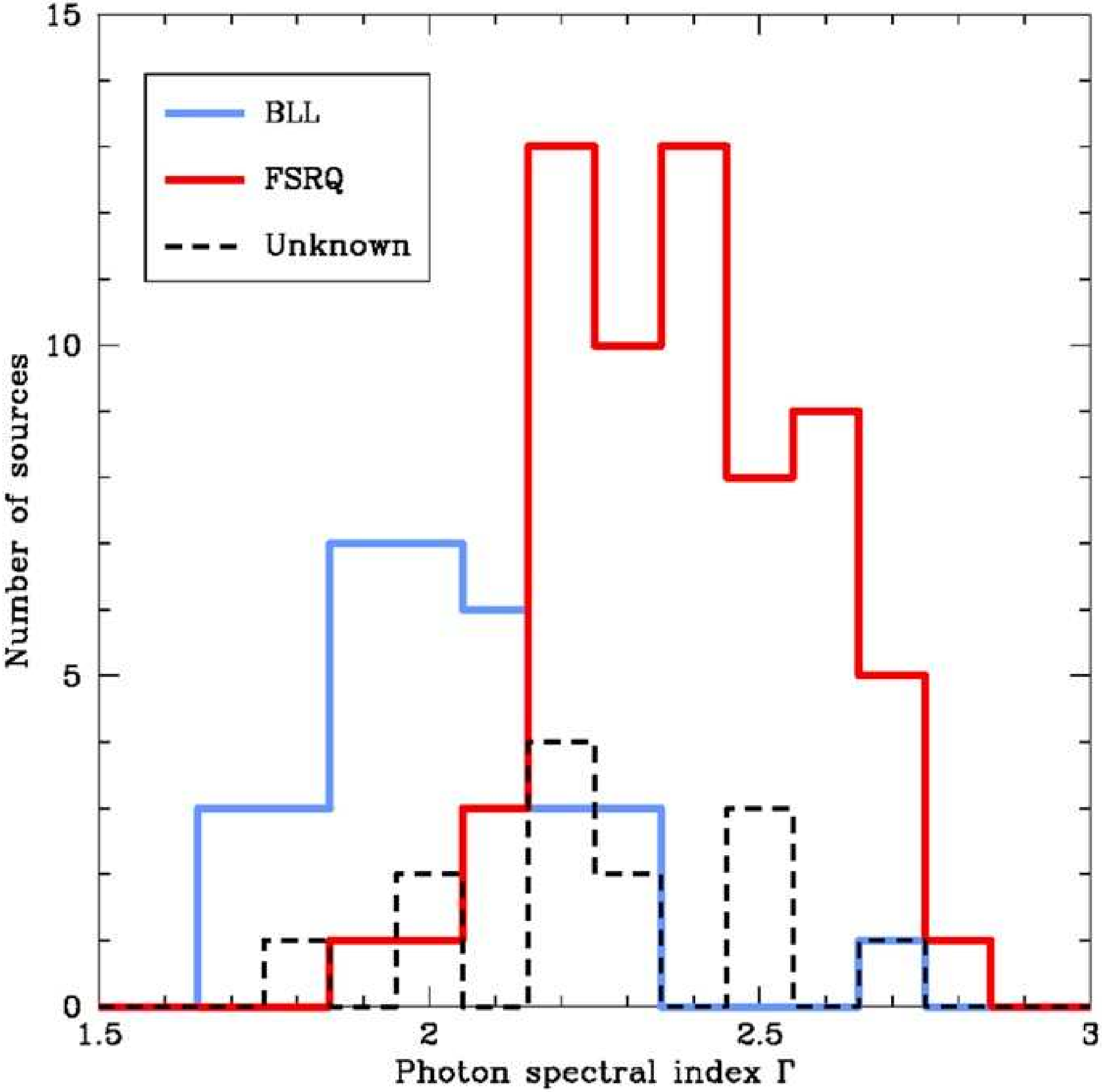

BLL
FSRQ
Unknown
Number of sources
Photon spectral index Γ
0
5
10
15
1.5
2
2.5
3

To be submitted to Astrophysical Journal

The Spectral Energy Distribution of *Fermi* bright blazars

Contact authors: P. Giommi, N. Mazziotta, E. Cavazzuti, S. Colafrancesco, S. Cutini, D. Gasparrini, C. Monte, S. Rainó, A. Tramacere

A. A. Abdo[1,2], M. Ackermann[3], M. Ajello[3], M. Axelsson[4,5], L. Baldini[6], J. Ballet[7], G. Barbiellini[8,9], D. Bastieri[10,11], B. M. Baughman[12], K. Bechtol[3], R. Bellazzini[6], B. Berenji[3], R. D. Blandford[3], E. D. Bloom[3], E. Bonamente[13,14], A. W. Borgland[3], J. Bregeon[6], A. Brez[6], M. Brigida[15,16], P. Bruel[17], T. H. Burnett[18], S. Buson[11], G. A. Caliandro[15,16], R. A. Cameron[3], P. A. Caraveo[19], J. M. Casandjian[7], E. Cavazzuti[20*], C. Cecchi[13,14], Ö. Çelik[22,23,24], A. Chekhtman[1,25], J. Chiang[3], S. Ciprini[13,14], R. Claus[3], J. Cohen-Tanugi[26], S. Colafrancesco[20*], L. R. Cominsky[27], J. Conrad[28,5,29], L. Costamante[3], S. Cutini[20*], C. D. Dermer[1], A. de Angelis[30], F. de Palma[15,16], S. W. Digel[3], E. do Couto e Silva[3], P. S. Drell[3], R. Dubois[3], D. Dumora[31,32], C. Farnier[26], C. Favuzzi[15,16], S. J. Fegan[17], W. B. Focke[3], P. Fortin[17], M. Frailis[30], L. Fuhrmann[33], Y. Fukazawa[34], S. Funk[3], P. Fusco[15,16], F. Gargano[16], D. Gasparrini[20*], N. Gehrels[22,35], S. Germani[13,14], B. Giebels[17], N. Giglietto[15,16], P. Giommi[20*], F. Giordano[15,16], T. Glanzman[3], G. Godfrey[3], I. A. Grenier[7], J. E. Grove[1], L. Guillemot[31,32], S. Guiriec[36], Y. Hanabata[34], A. K. Harding[22], M. Hayashida[3], E. Hays[22], S. E. Healey[3], R. E. Hughes[12], R. Itoh[34], M. S. Jackson[28,5,37], G. Jóhannesson[3], A. S. Johnson[3], W. N. Johnson[1], M. Kadler[38,23,39,40], T. Kamae[3], H. Katagiri[34], J. Kataoka[41,42], N. Kawai[41,43], M. Kerr[18], J. Knödlseder[44], M. L. Kocian[3], Y. Y. Kovalev[45,33], M. Kuss[6], J. Lande[3], L. Latronico[6], F. Longo[8,9], F. Loparco[15,16], B. Lott[31,32], M. N. Lovellette[1], P. Lubrano[13,14], G. M. Madejski[3], A. Makeev[1,25], W. Max-Moerbeck[46], M. N. Mazziotta[16*], W. McConville[22,35], J. E. McEnery[22]

Quasi simultaneous SEDs for 48 LBAS blazars

- Data from Fermi, Swift, Effelsberg, OVRO, RATAN, TANAMI-VLBI, GASP-WEBT collaboration, VLT-VISIR, Spitzer, AGILE
- Fermi data integrated between 4 August to 31 October 2008.
- Quasi-simultanaous multi-frequency data taken in the interval May 2008 January 2009.
- Archival multi-frequency data (radio to TeV)

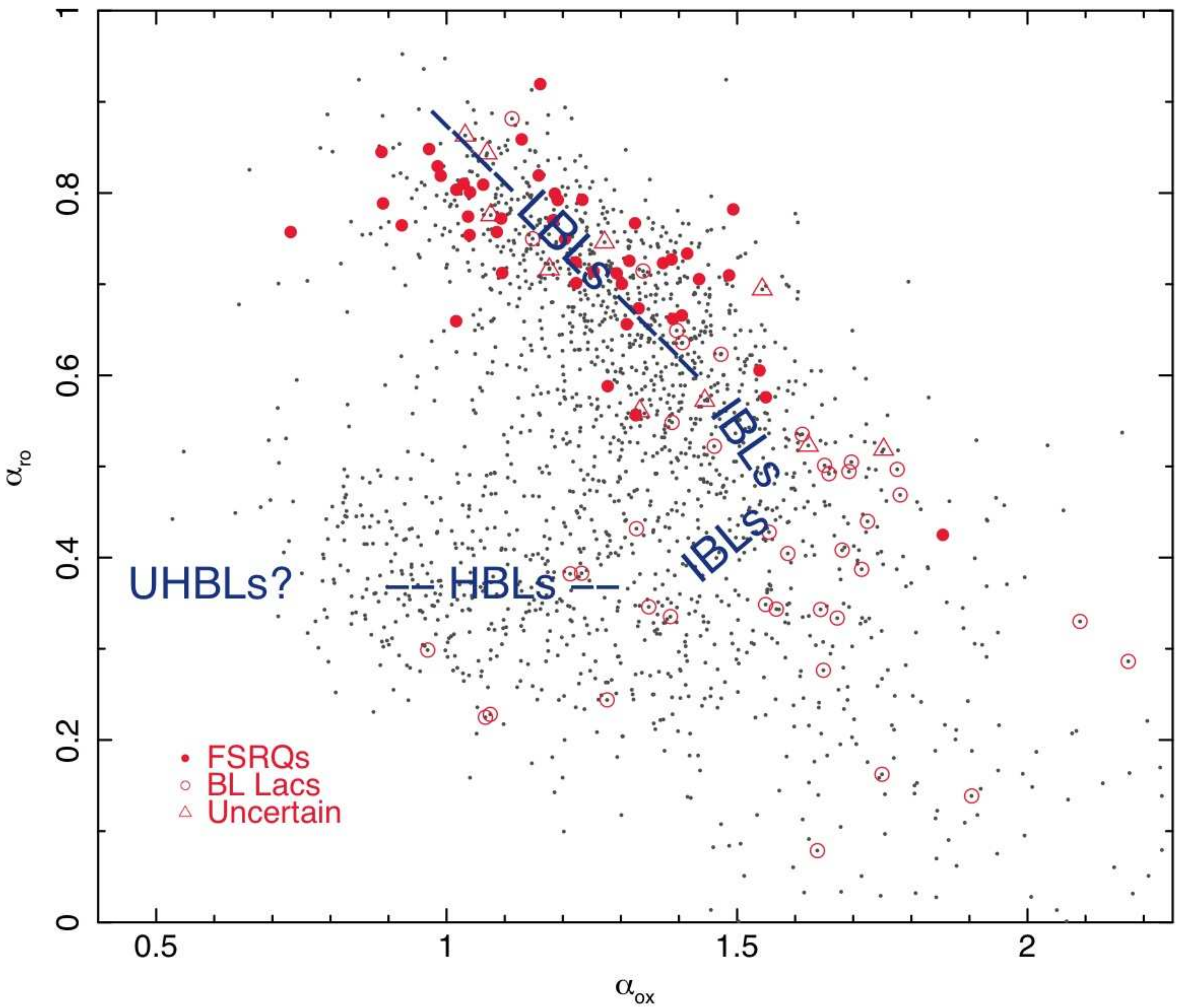

1
0.8
0.6
0.4
0.2
0
0.5
1
1.5
2
α_ro
α_ox
LBLs
IBLs
IBLs
UHBLs?
HBLs
FSRQs
BL Lacs
Uncertain

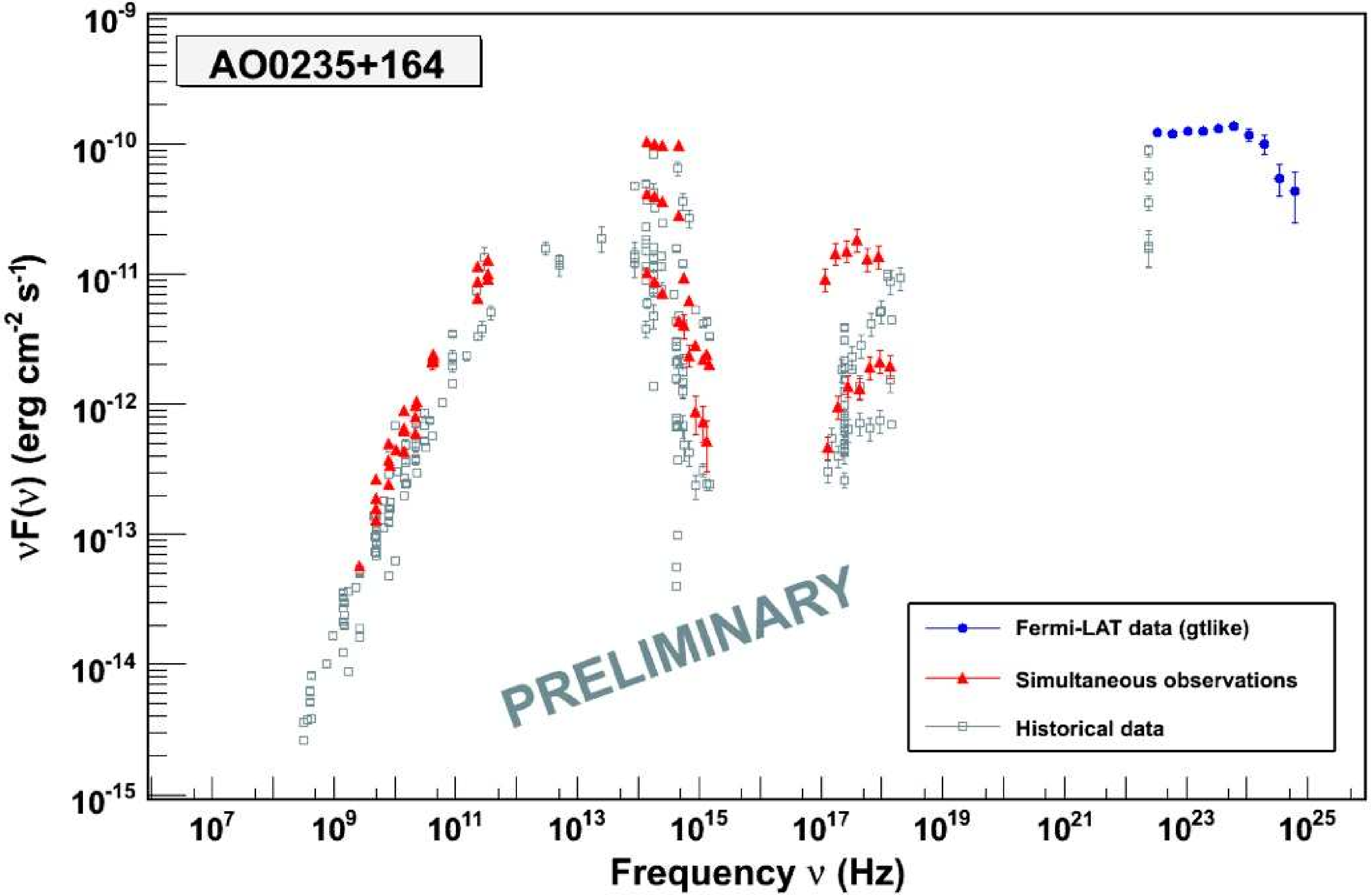
AO0235+164
PRELIMINARY
Fermi-LAT data (gtlike)
Simultaneous observations
Historical data
νF(ν) (erg cm-2 s-1)
Frequency ν (Hz)
10-9
10-10
10-11
10-12
10-13
10-14
10-15
10^7
10^9
10^11
10^13
10^15
10^17
10^19
10^21
10^23
10^25

The synchrotron/invC peak frequencies ν_{peak} and intensities $\nu_{peak}\, f(\nu_{peak})$

Measured from the 48 SEDs using
3rd degree polynomial functions

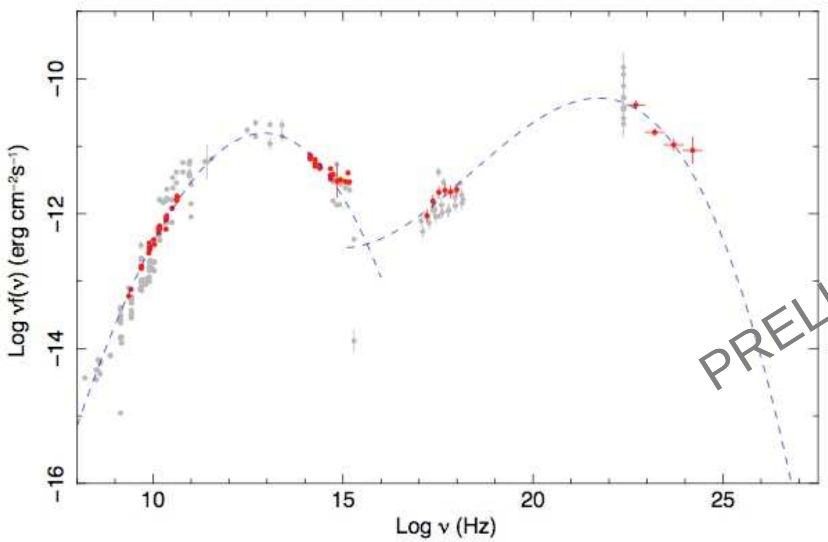

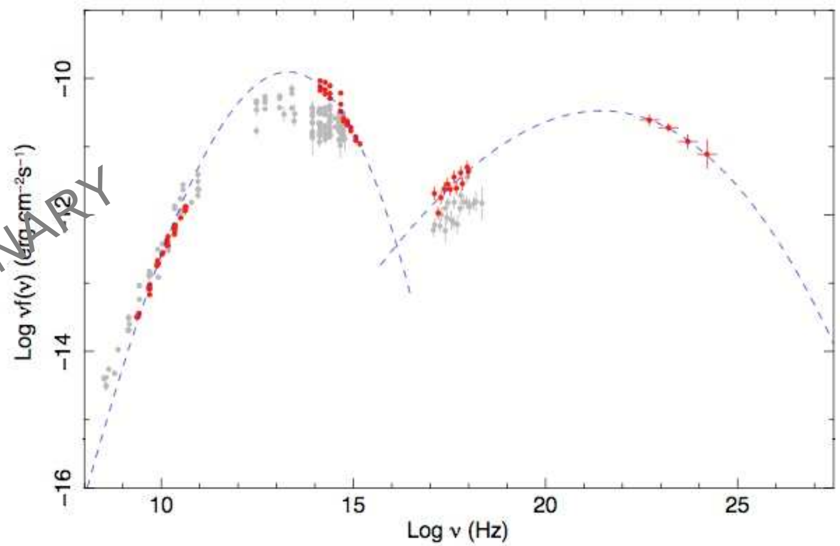

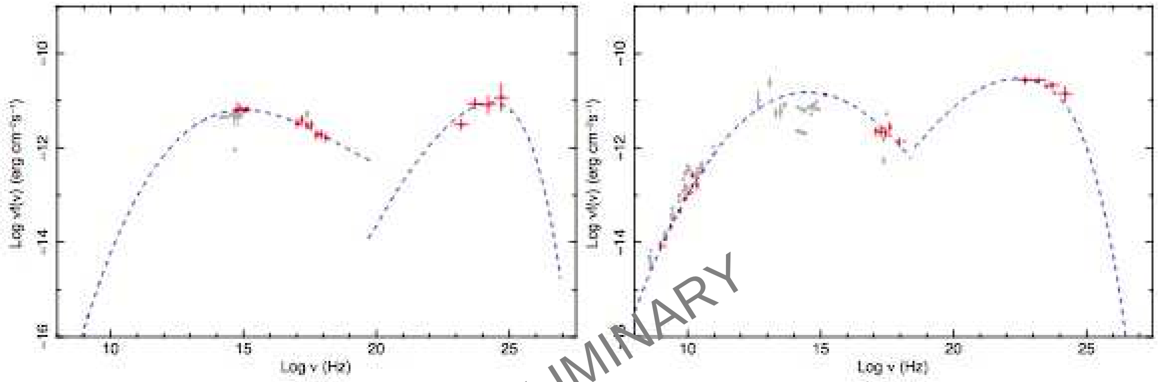

Fig. 3.— The SED of 0FGL J0033.6-1921 = 1RXS J003334.6-192130 = SHBL J003334.2-192133 (left) and of 0FGL J0050.5-0928 = PKS0048-09 (right)

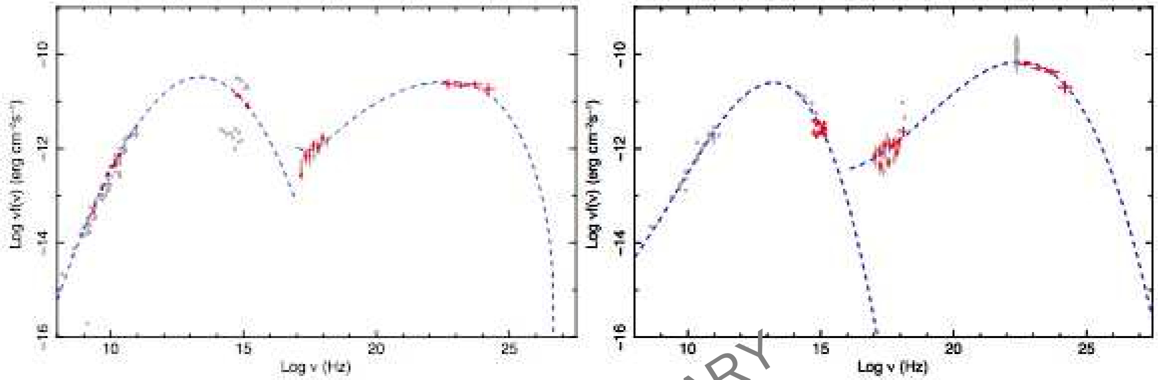

Fig. 4.— The SED of 0FGL J0137.1+4751 = S40133+47 (left) and of 0FGL J0210.8-5100 = PKS0208-512 (right)

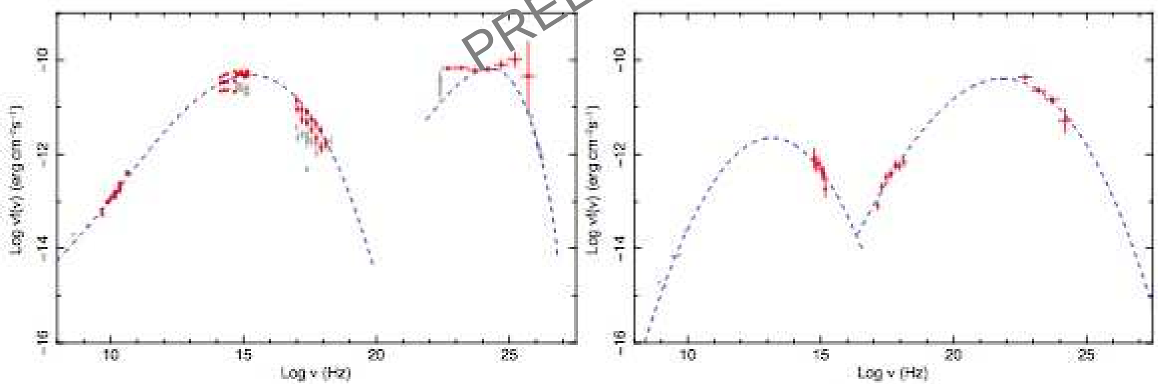

Fig. 5.— The SED of 0FGL J0222.6+4302 = 3C 66A (left) and of 0FGL J0229.5-3640 = PKS0227-369 (right)

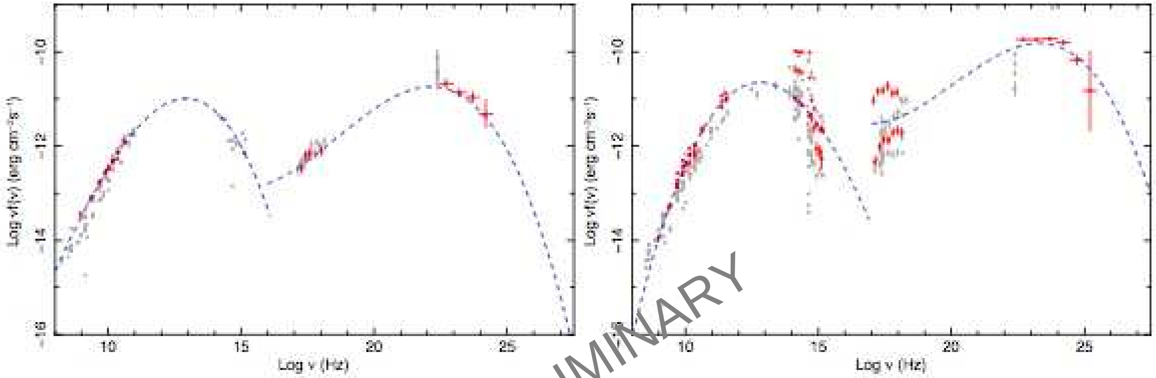

Fig. 6.— The SED of 0FGL J0238.4+2855 = 4C28.07 (left) and of 0FGL J0238.6+1636 = PKS0235+164 (right).

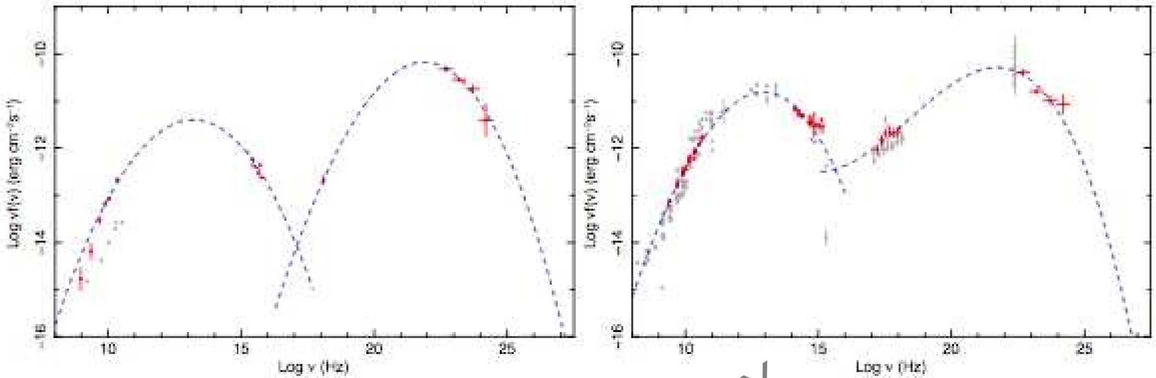

Fig. 7.— The SED of 0FGL J0349.8-2102 = PKS 0347-211 (left) and of 0FGL J0423.1-0112 = PKS0420-01 (right)

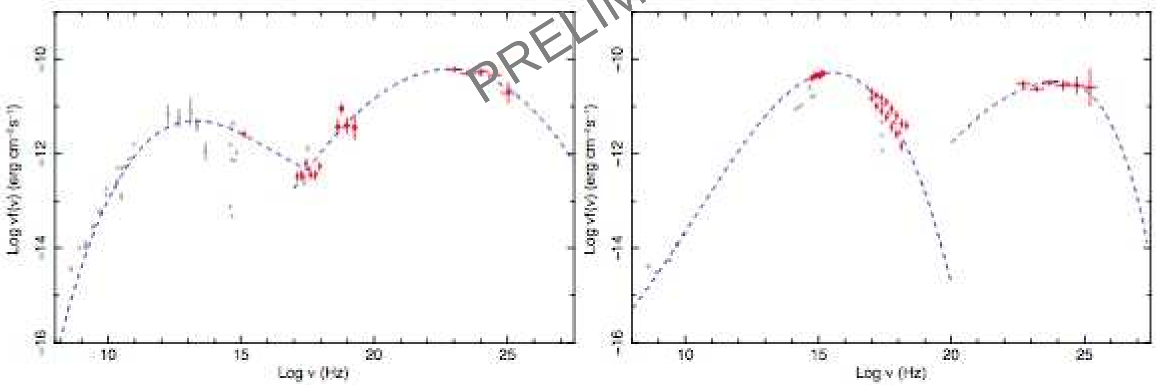

Fig. 8.— The SED of 0FGL J0428.7-3755 = PKS0426-380 (left) and of 0FGL J0449.7-4348 = PKS0447-439 (right)

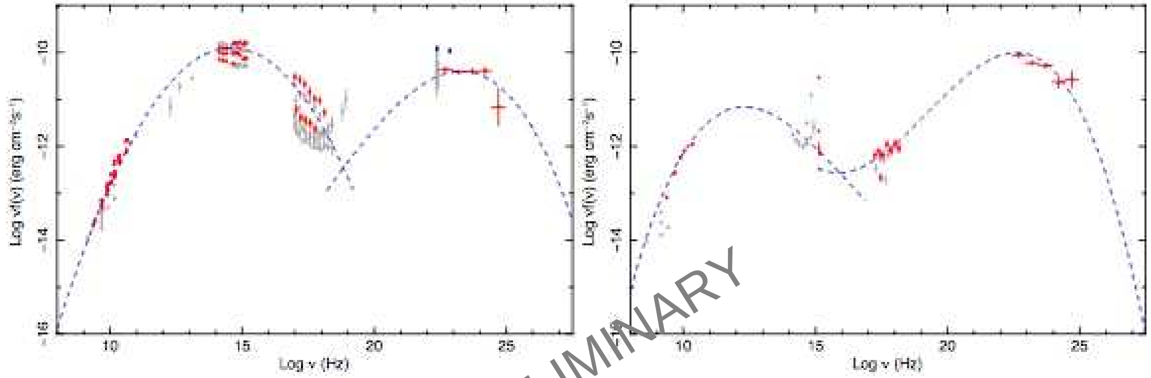

Fig. 12.— The SED of 0FGL J0722.0+7120 = S50716+714 (left) and of 0FGL J0730.4-1142 = PKS0727-11 (right)

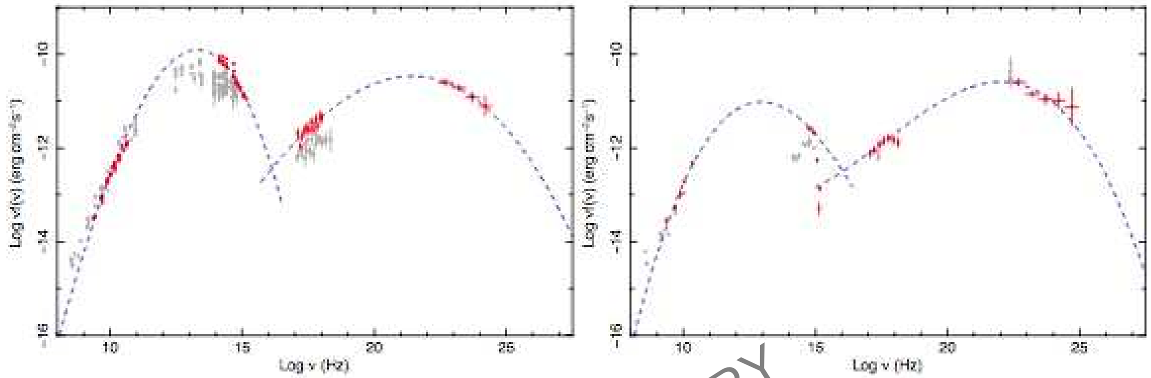

Fig. 13.— The SED of 0FGL J0855.4+2009 = PKS0851+202 (left) and of 0FGL J0921.2+4437 = S40917+44 (right)

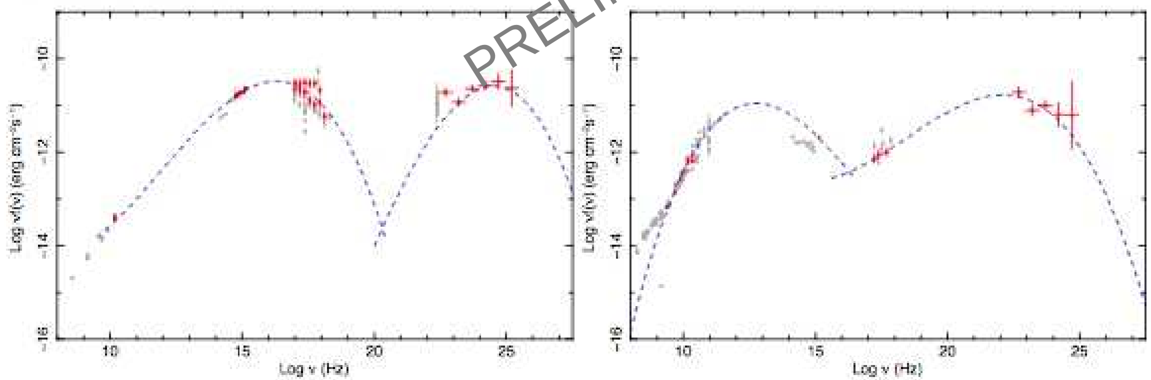

Fig. 14.— The SED of 0FGL J1015.2+4927 = 1H 1013+498 (left) and of 0FGL J1057.8+0138 = 4C01.28 (right)

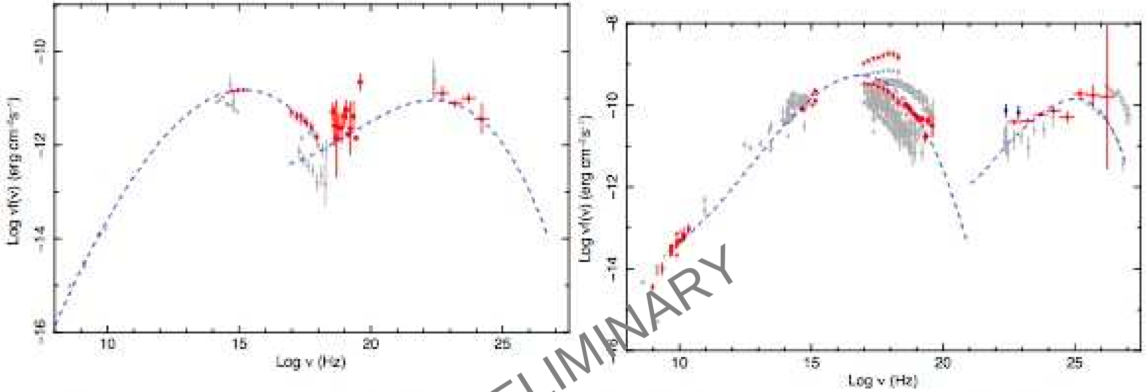

Fig. 15.— The SED of 0FGL J1058.9+5629 = GB6 J1058+5628 (left) and of 0FGL J1104.5+3811 = Mkn 421 (right)

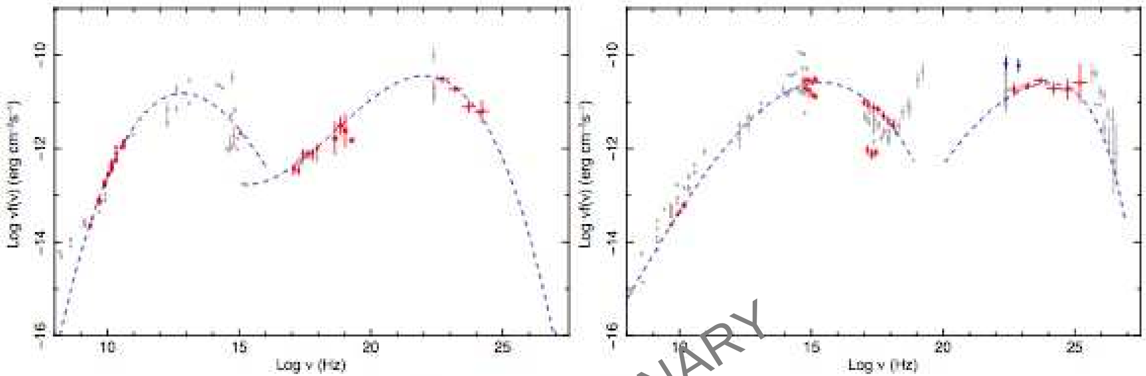

Fig. 16.— The SED of 0FGL J1159.2+2912 = 4C29.45 (left) and of 0FGL J1221.7+2814 = ON231= W Comae (right)

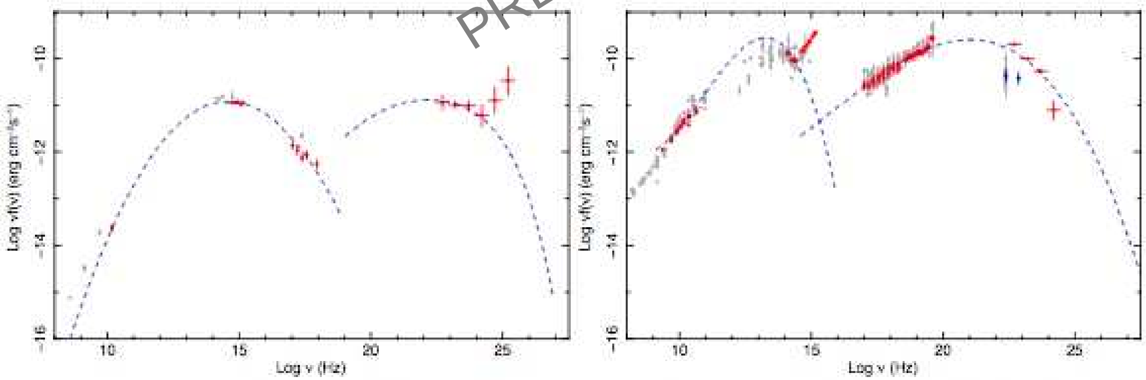

Fig. 17.— The SED of 0FGL J1248.7+5811 = PG 1246+586 (left) and of 0FGL J1229.1+0202 = 3C273 (right)

A method to derive ν^S_{peak} and ν^S_{peak} f(ν^S_{peak}) form α_{ox} and α_{ro}

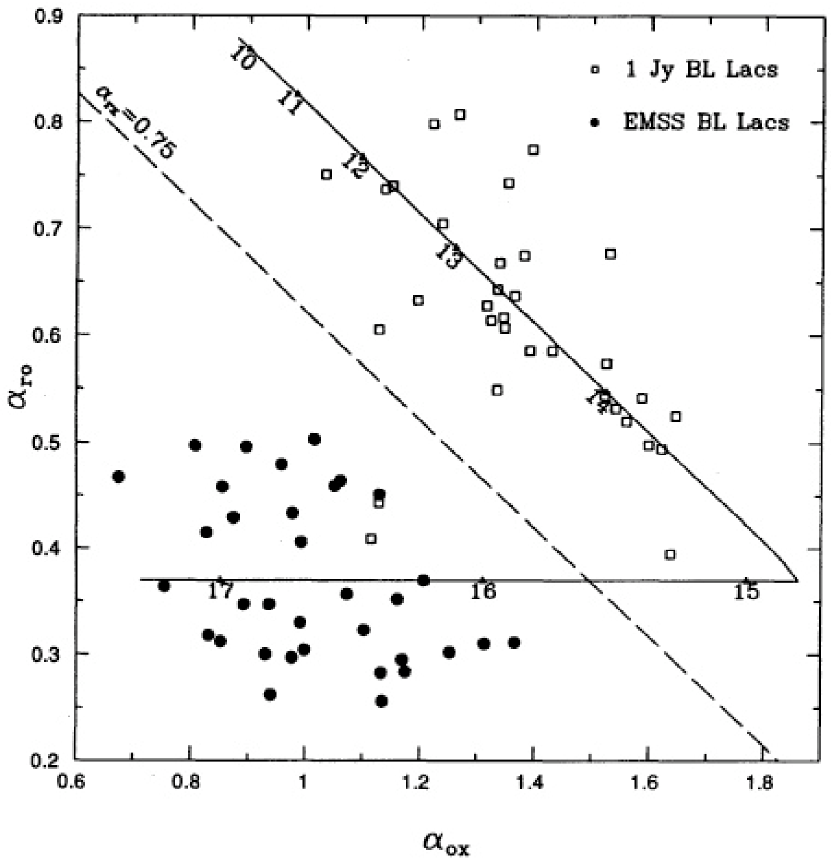

A "calibrated" version of the method of Padovani & Giommi (1995)

The position of a blazar in the α_{ox} - α_{ro} plane is determined by the synchrotron peak energy

Paodvani & Giommi 1995, ApJ, 444, 567

$$\mathrm{Log}(\nu_{peak_S}) = \begin{cases} 13.85 + 2.30X & if \quad \mathrm{X} < 0 \text{ and } \mathrm{Y} < 0.3 \\ 13.15 + 6.58Y & \text{otherwise} \end{cases}$$

where $\mathrm{X} = 0.565 - 1.433 \cdot \alpha_{\rm ro} + 0.155 \cdot \alpha_{\rm ox}$ and $\mathrm{Y} = 1.0 - 0.661 \cdot \alpha_{\rm ro} - 0.339 \cdot \alpha_{\rm ox}$

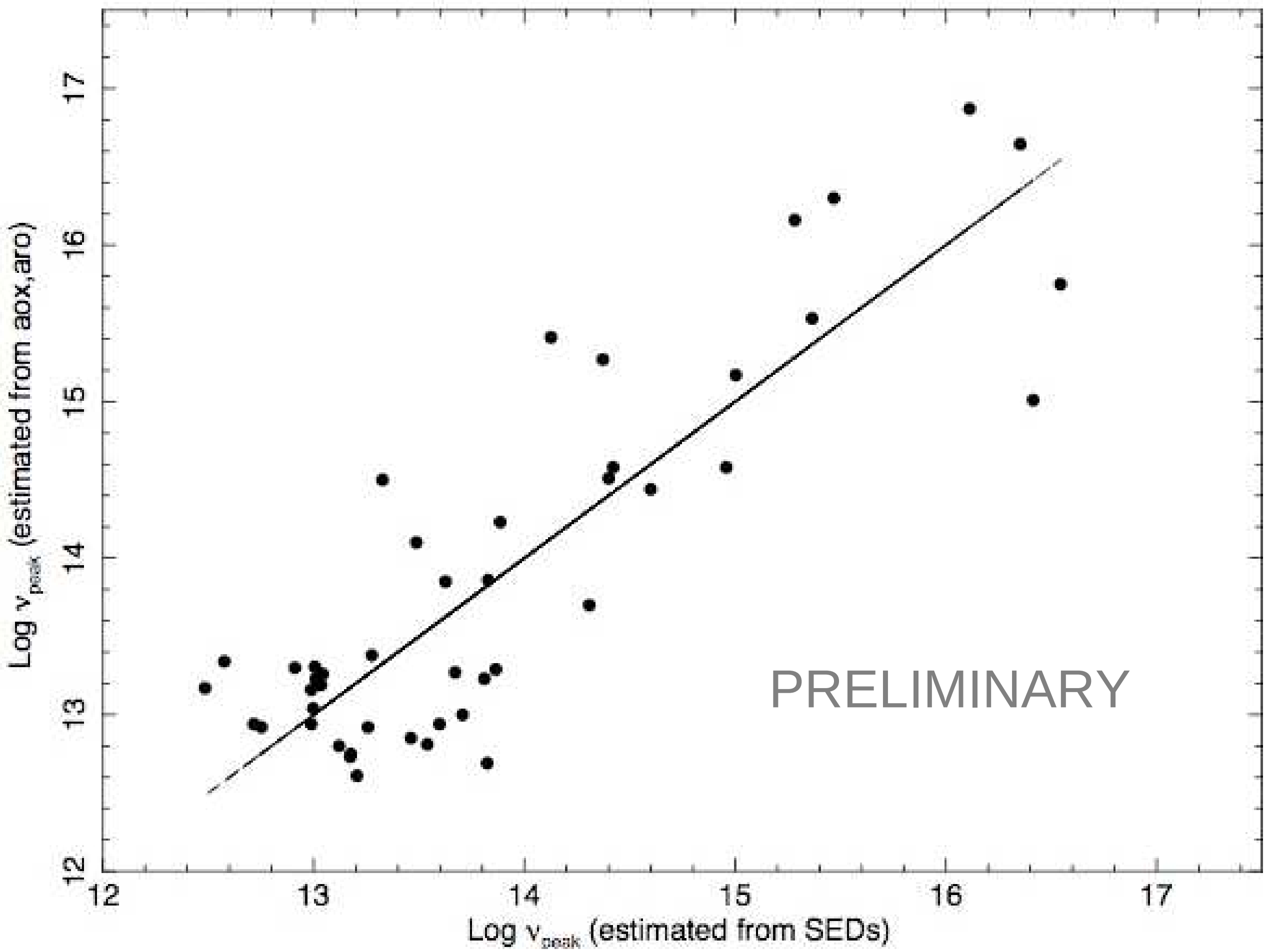

$$\mathrm{Log}(\nu_{peak_S} F(\nu_{peak_S})) = 0.5 \cdot \mathrm{Log}(\nu_{peakS}) - 20.4 + 0.9 \cdot \mathrm{Log}(\mathrm{Rflux}),$$

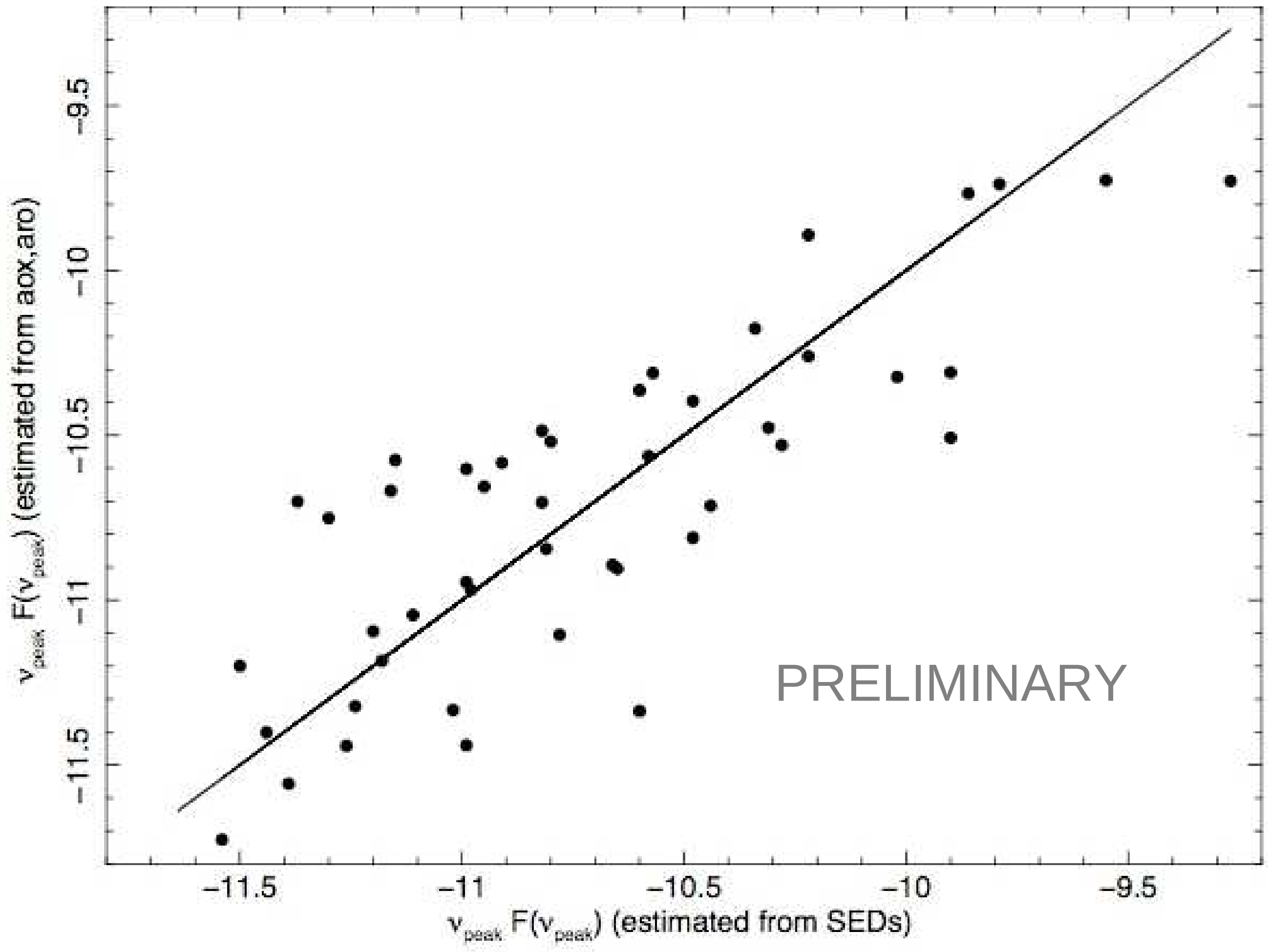

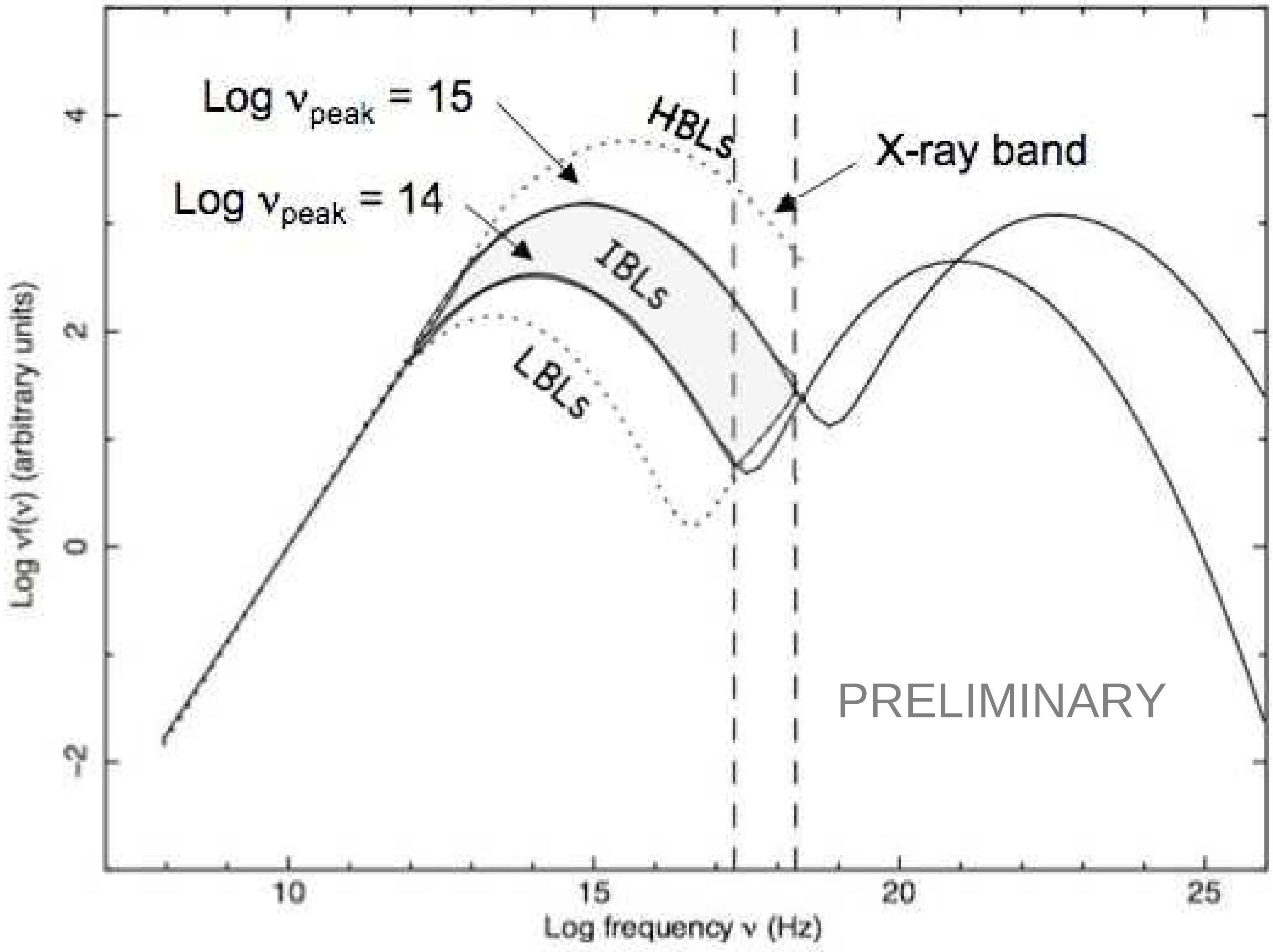
Log ν_{peak} = 15
Log ν_{peak} = 14
HBLs
IBLs
LBLs
X-ray band
PRELIMINARY
Log νf(ν) (arbitrary units)
Log frequency ν (Hz)
4
2
0
-2
10
15
20
25

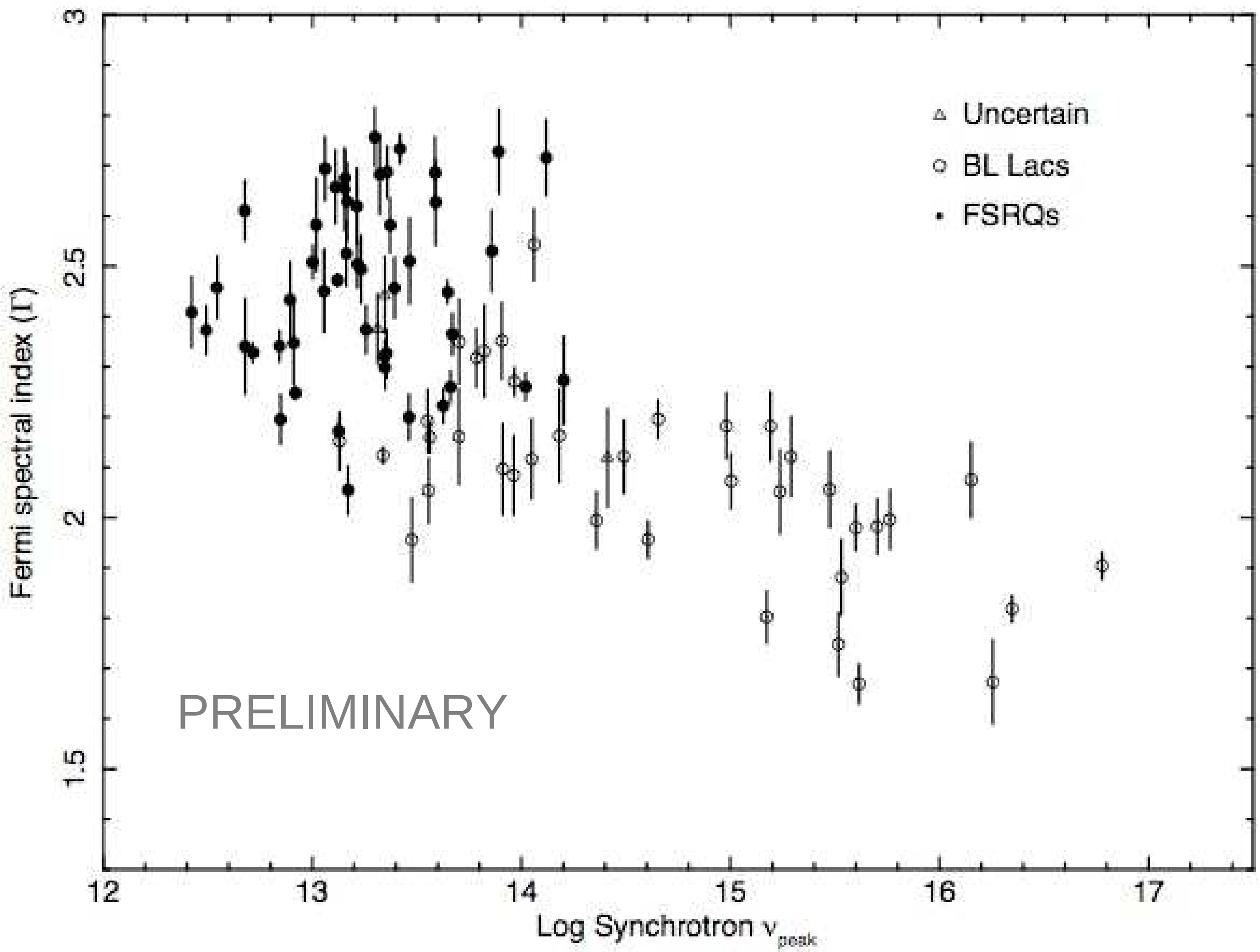

Fermi spectral index (Γ)
Log Synchrotron ν_{peak}
Uncertain
BL Lacs
FSRQs
PRELIMINARY
3
2.5
2
1.5
12
13
14
15
16
17

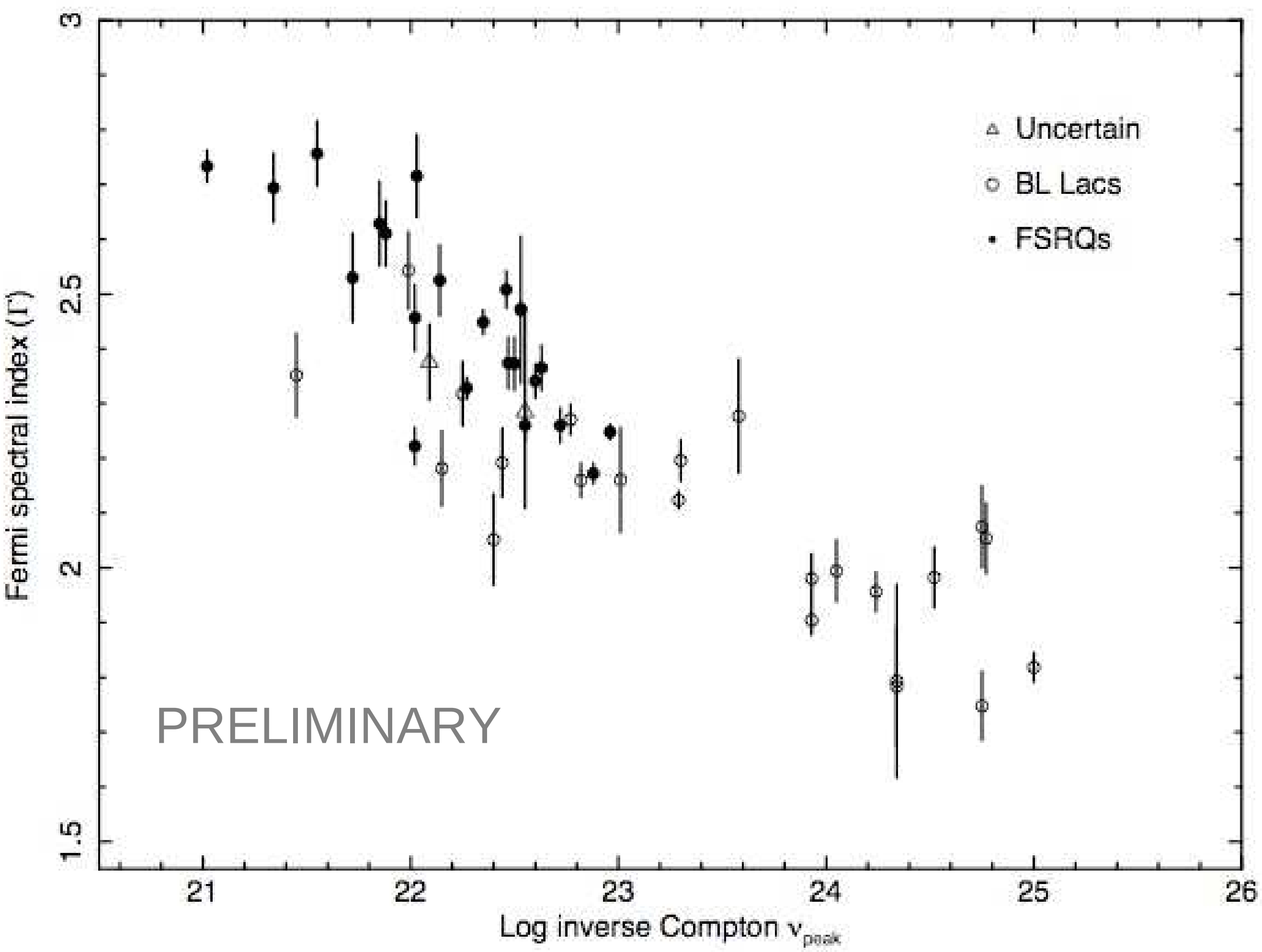
Uncertain
BL Lacs
FSRQs
PRELIMINARY
Fermi spectral index (Γ)
Log inverse Compton ν_peak
1.5
2
2.5
3
21
22
23
24
25
26

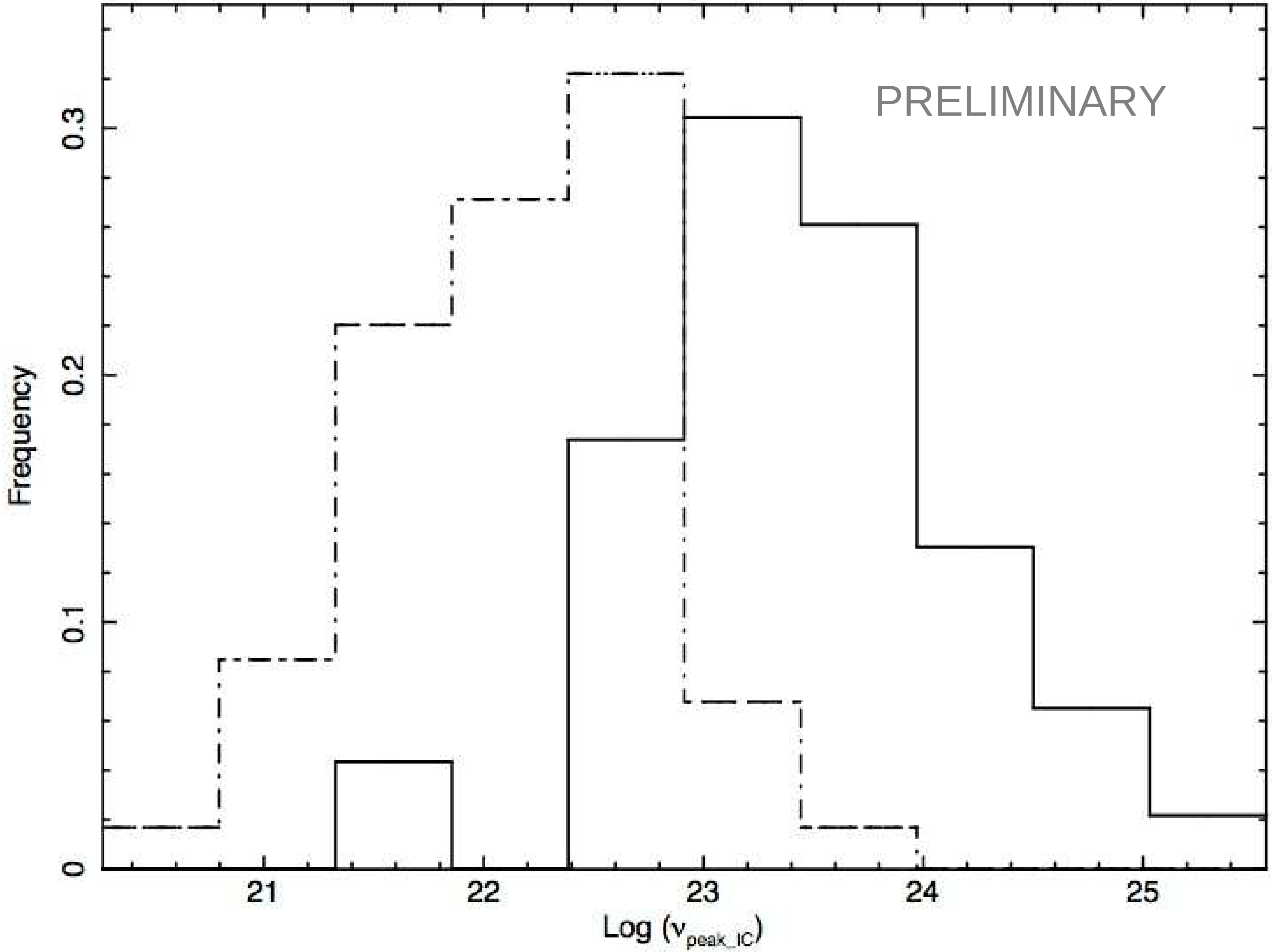

Fig. 35.— The distribution of inverse Compton peak frequency for the sample of LBAS FSRQ (dot-dashed line) and BL Lacs (solid line).

Table 13. Blazar SED parameters

Name 0FGL (1)	SED available (2)	α_r (3)*	$Log(\nu^S_{peak})$ (4)**	$Log(\nu^S_{peak} F(\nu^S_{peak}))$ (5)**	$Log(\nu^{IC}_{peak})$ (6)***	$Log(\nu^{IC}_{peak} F(\nu^{IC}_{peak}))$ (7)	$Log(\gamma^{SSC}_{peak})$ (8)****	Compton dominance (9)	Blazar type (10)
J0017.4−0503	-	0.127	−−/13.6	−−/-11.4	-/20.7	-	3.4	-	FSRQ - LBL
J0033.6−1921	Yes	0	16.1/16.3	-11.1/-11.2	24.3/24.8	-11.1	4	1	BL Lac - HBL
J0050.5−0928	Yes	0.205	14.3/14.4	-10.8/-10.6	22.4/23	-10.6	4	1.8	BL Lac - IBL
J0051.1−0647	-	-0.103	−−/12.8	−−/-11.4	-/22.7	-	4.8	-	FSRQ - LBL
J0112.1+2247	-	0.121	−−/14.6	−−/-10.8	-/23.1	-	4.1	-	BL Lac - IBL
J0118.7−2139	-	0.089	−−/13	−−/-11.5	-/22.3	-	4.5	-	FSRQ - LBL
J0120.5−2703	-	-0.114	−−/13.9	−−/-10.8	-/23.6	-	4.7	-	BL Lac - LBL
J0136.6+3903	-	0	−−/16	−−/-10.9	-/24.9	-	4.4	-	BL Lac - HBL
J0137.1+4751	Yes	0.192	13.6/13.3	-10.5/-10.8	22.6/22.8	-10.6	4.4	0.8	FSRQ - LBL
J0144.5+2709	-	0.011	−−/−−	−−/−−	-/22.7	-	-	-	BL Lac
J0145.1−2728	-	-0.199	−−/13.3	−−/-11.2	-/21.4	-	3.9	-	FSRQ - LBL
J0204.8−1704	-	-0.017	−−/13.3	−−/-11	-/21.6	-	4.1	-	FSRQ - LBL
J0210.8−5100	Yes	-0.099	12.5/13.8	-10.7/-10.4	22.4/22.[illegible]	-10.2	4.8	3.6	FSRQ - LBL
J0217.8+0146	-	0.237	−−/12.9	−−/-11.1	-/23	-	5	-	FSRQ - LBL
J0220.9+3607	-	-0.186	−−/12.4	−−/-11.4	-/2[illegible]	-	4.3	-	FSRQ - LBL
J0222.6+4302	Yes	0	15.1/14.4	-10.2/-10.6	24.[illegible]/23.7	-10.2	4.4	1	BL Lac - IBL
J0229.5−3640	Yes	0	13.5/13	-11.7/-12	21.8/21.3	-10.4	4.1	20.3	FSRQ - LBL
J0238.4+2855	Yes	0.126	12.8/12.8	-10.7/-11	[illegible]/21.6	-10.8	4.6	0.9	FSRQ - LBL
J0238.6+1636	Yes	0.557	13.5/13.1	-10/-10.9	[illegible].2/23.3	-9.9	4.8	1.5	BL Lac - LBL
J0245.6−4656	-	-0.397	−−/−−	−−/−−	-/22.2	-	-	-	BZU
J0303.7−2410	-	-0.664	−−/15.1	−−/-10.6	-/23.5	-	4.1	-	BL Lac - HBL
J0334.1−4006	-	-0.036	−−/13.3	−−/-11	-/23	-	4.8	-	BL Lac - LBL
J0349.8−2102	Yes	0.014	12.9/13	-11.3/-11.6	21.8/21.3	-10.2	4.4	13.5	FSRQ - LBL
J0423.1−0112	Yes	-0.081	13.4/13.3	-10.9/-10.5	21.7/22	-10.3	4	4.1	FSRQ - LBL
J0428.7−3755	Yes	0.419	13.3/13.6	-11/-10.8	22.8/23	-10.2	4.6	6.3	BL Lac - LBL
J0449.7−4348	Yes	-0.498	15.6/15.4	-10.2/-10.[illegible]	23.9/23.5	-10.5	4.1	0.5	BL Lac - HBL
J0457.1−2325	Yes	-0.074	13.1/13	-11/-11	22.8/22.6	-9.9	4.7	12.5	FSRQ - LBL
J0507.9+6739	Yes	0	16.6/16.3	-10.7/-11	24.3/24.9	-10.5	3.7	1.4	BL Lac - HBL
J0516.2−6200	Yes	0.226	13.6/13	-11.3/-11.5	22.5/22.9	-10.7	4.4	4.1	BZU - LBL
J0531.0+1331	Yes	0.239	12.8/13.1	-10.9/-10.7	21.3/21.4	-9.8	4.2	11.6	FSRQ - LBL
J0538.8−4403	Yes	-0.084	13.4/13.6	-10.6/-10.3	22.7/22.8	-10.1	4.6	3.6	BL Lac - LBL
J0654.3+5042	-	0.231	−−/−−	−−/−−	-/23.5	-	-	-	BZU
J0654.3+4513	-	0.005	−−/13	−−/-11.6	-/22.3	-	4.6	-	FSRQ - LBL
J0700.0−6611	-	-0.173	−−/−−	−−/−−	-/23.6	-	-	-	BZU
J0712.9+5034	Yes	0.403	13.6/14.3	-11.3/-11.4	23/23.4	-11	4.6	2.1	BL Lac - IBL
J0714.2+1934	-	0	−−/−−	−−/−−	-/22.1	-	-	-	BZU
J0719.4+3302	-	-0.149	−−/13.6	−−/-11.4	-/22.1	-	4.2	-	FSRQ - LBL
J0722.0+7120	Yes	-0.126	14.6/14.4	-9.9/-10.6	23.3/23.2	-10.4	4.2	0.3	BL Lac - IBL
J0738.2+1738	-	0.271	−−/13.8	−−/-10.6	-/23.1	-	4.6	-	BL Lac - LBL
J0818.3+4222	-	-0.042	−−/12.6	−−/-11.2	-/23.3	-	5.2	-	BL Lac - LBL
J0824.9+5551	-	0.095	−−/13	−−/-11.2	-/20.3	-	3.5	-	FSRQ - LBL
J0855.4+2009	Yes	0.443	13.4/13.9	-9.8/-10.4	21.4/22.3	-10.5	3.9	0.2	BL Lac - LBL

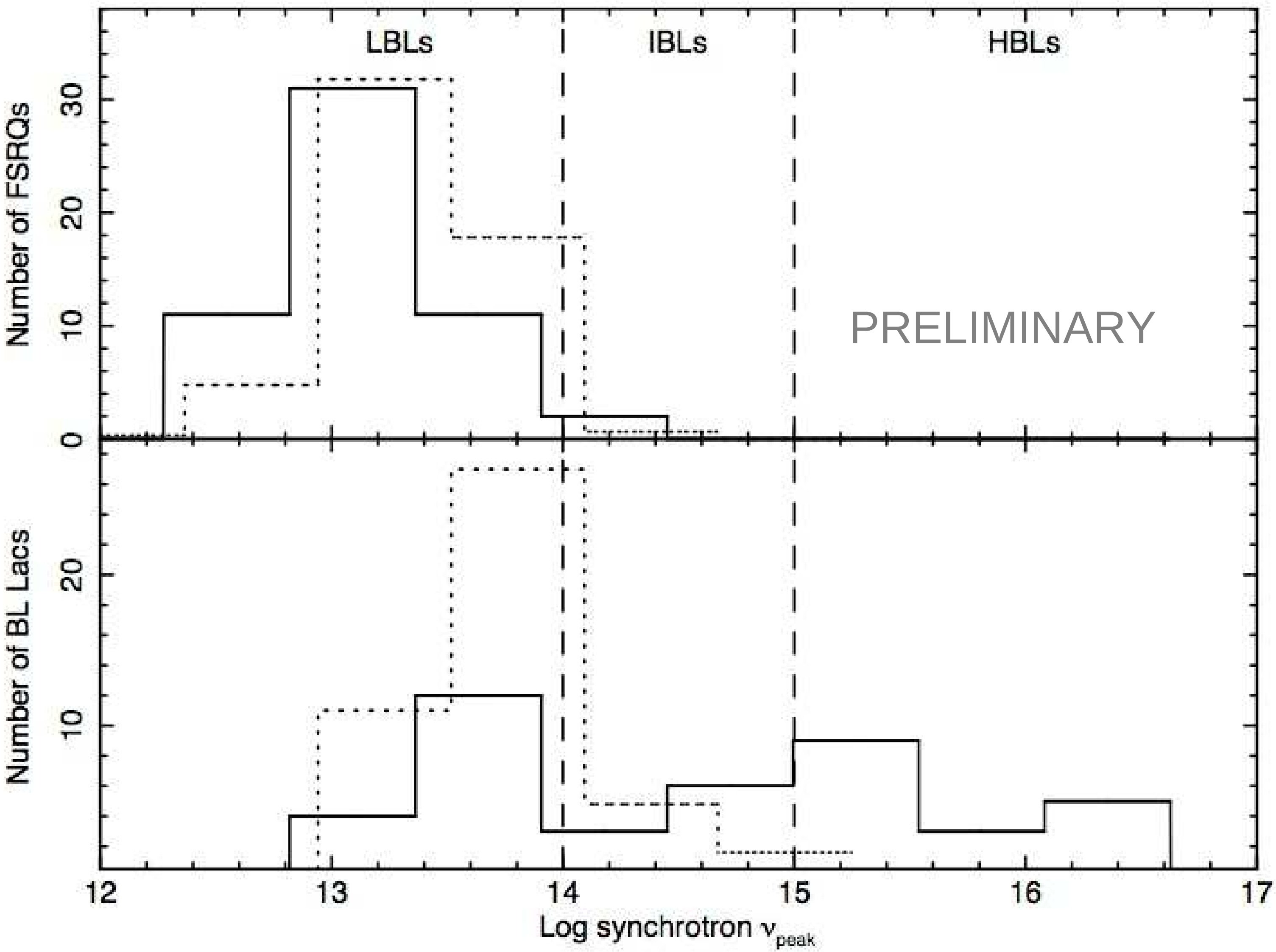

Fig. 33.— The distribution of synchrotron peak energy for the sample of LBAS FSRQ (solid line, top panel) and BL Lacs (solid line, bottom panel) compared to that of microwave selected blazars listed in the WMAP foreground sources catalog (dotted histograms) . The WMAP counts have been scaled to match the LBAS sample.

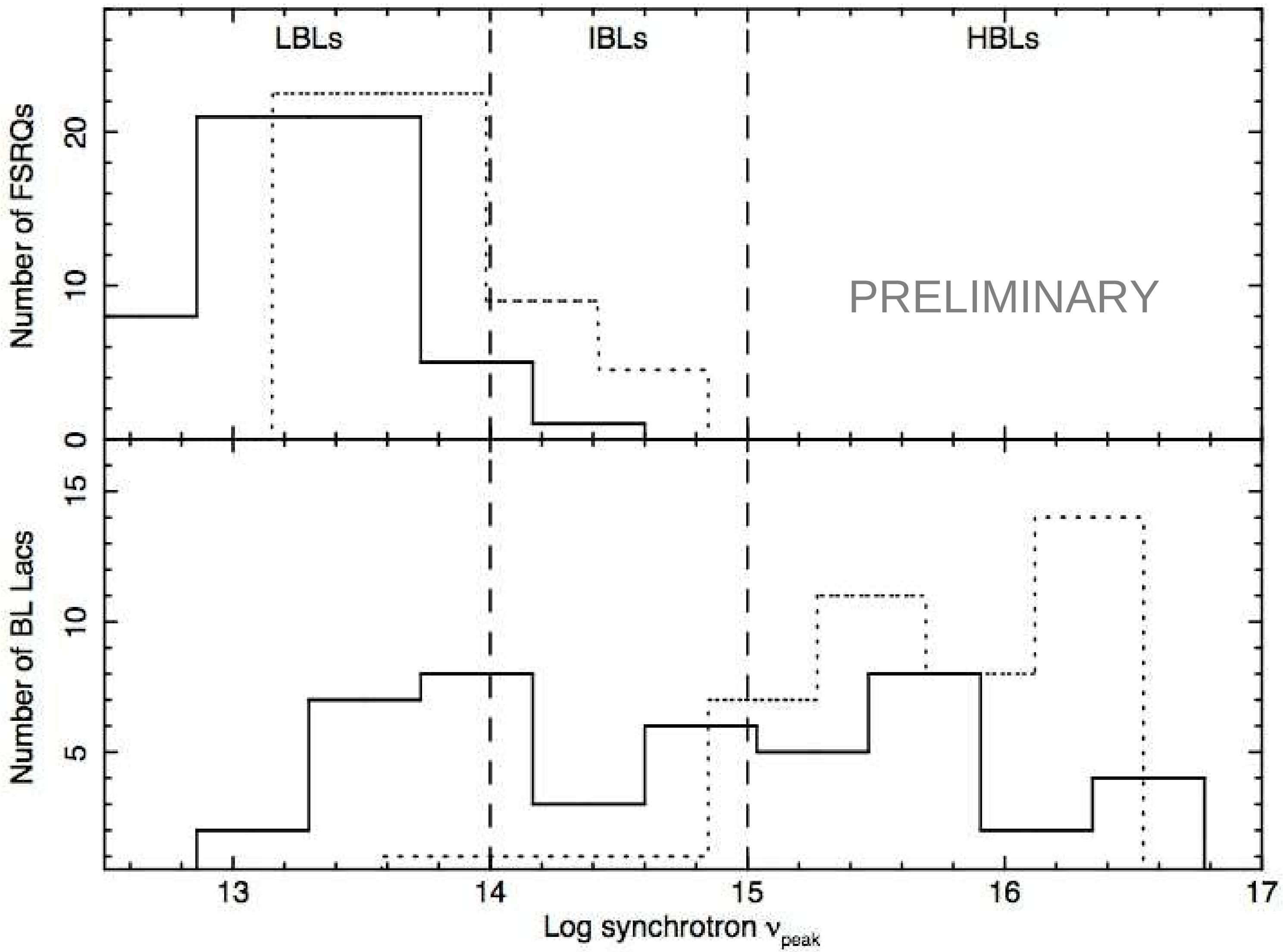

Fig. 34.— The distribution of synchrotron peak energy for the sample of LBAS FSRQ (solid line, top panel) and BL Lacs (solid line, bottom panel) compared to that of the sample of X-ray selected blazars of the *Einstein* Extended Medium Sensitivity Survey (EMSS, dotted histograms). The EMSS counts have been scaled to match the LBAS sample.

Fermi LBAS

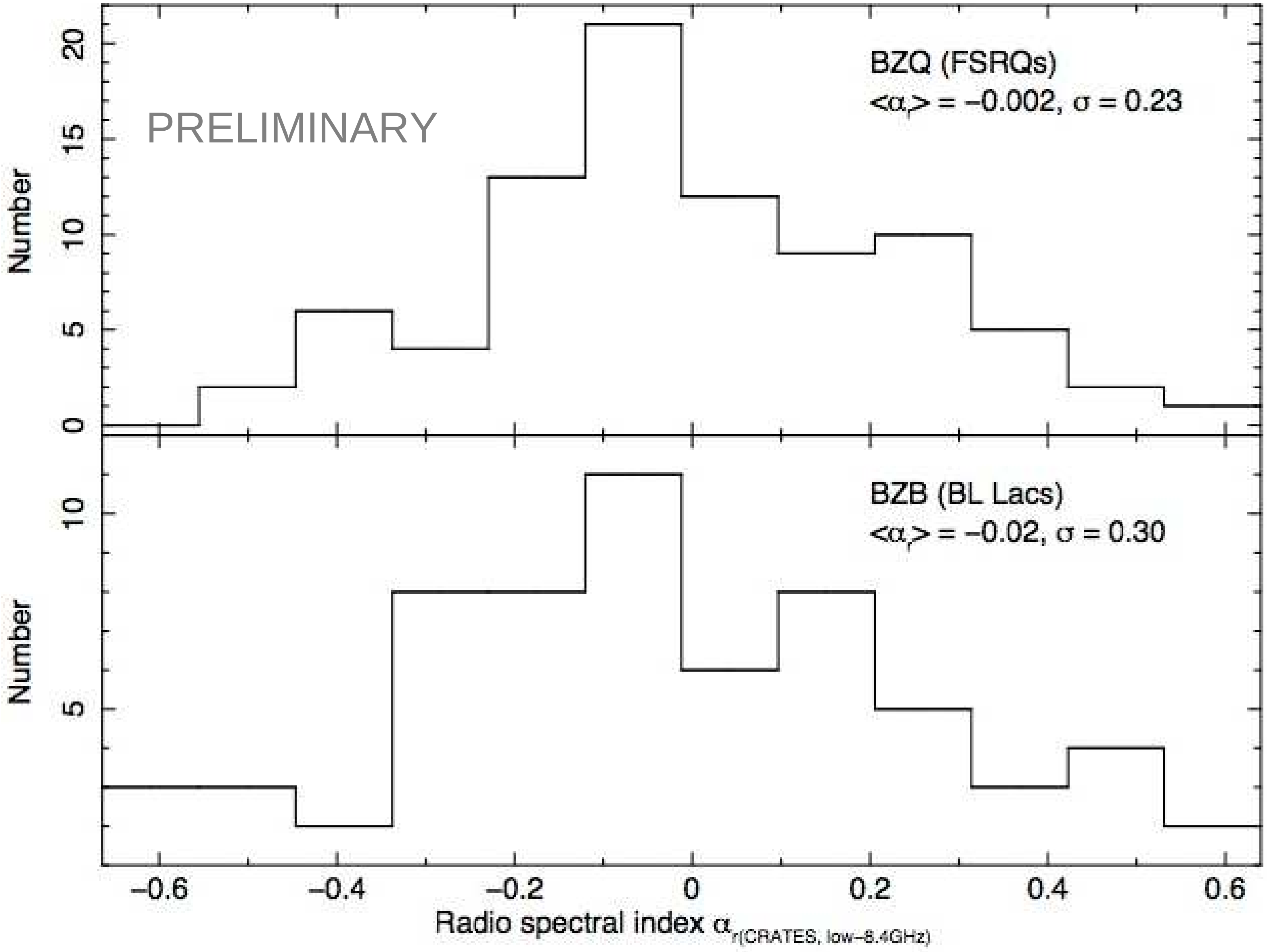

PRELIMINARY
BZQ (FSRQs)
<α_r> = −0.002, σ = 0.23
BZB (BL Lacs)
<α_r> = −0.02, σ = 0.30
Number
Number
Radio spectral index α_r(CRATES, low−8.4GHz)
−0.6
−0.4
−0.2
0
0.2
0.4
0.6
0
5
10
15
20
5
10

WMAP-5yr foreground Blazars

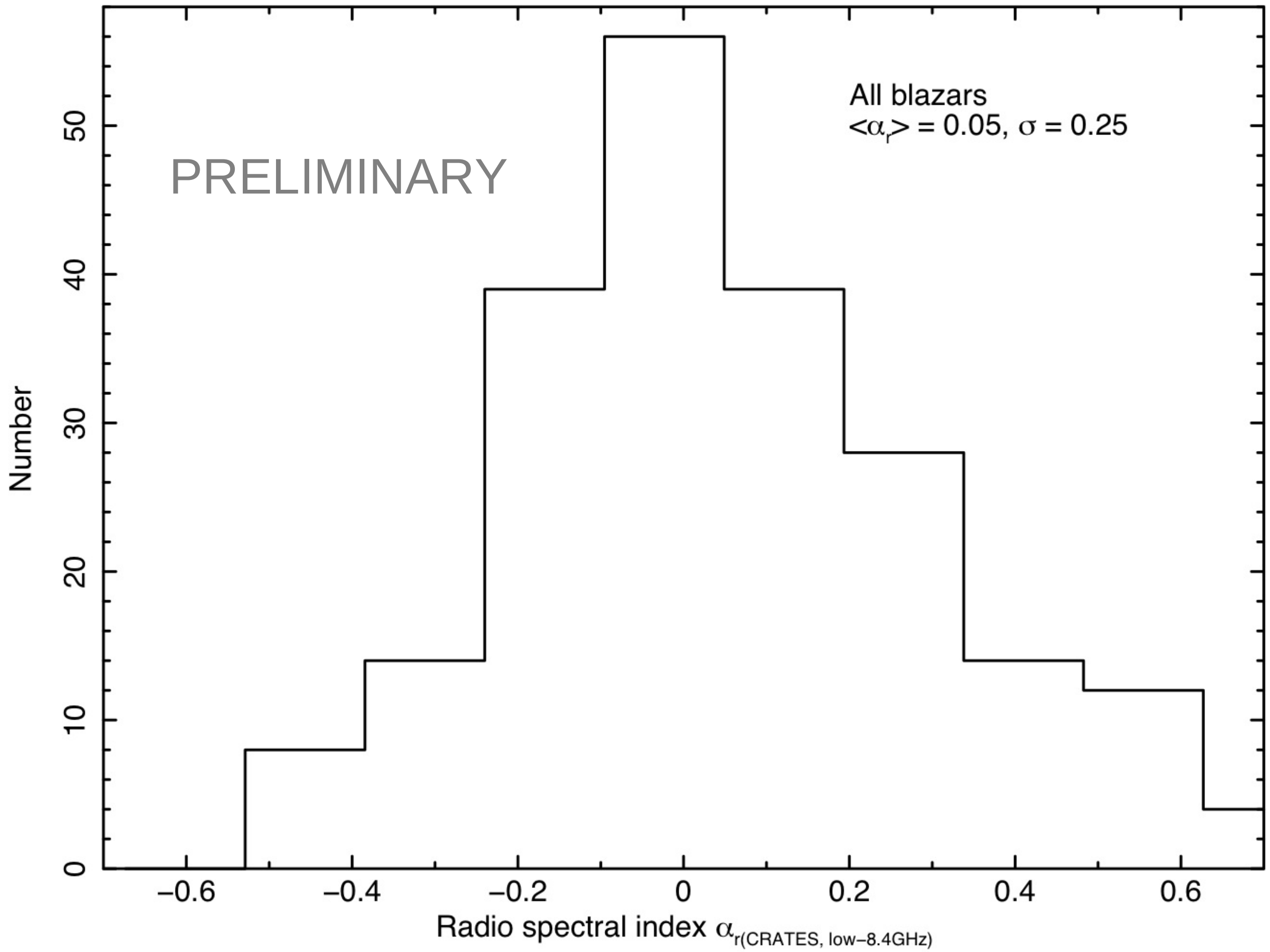

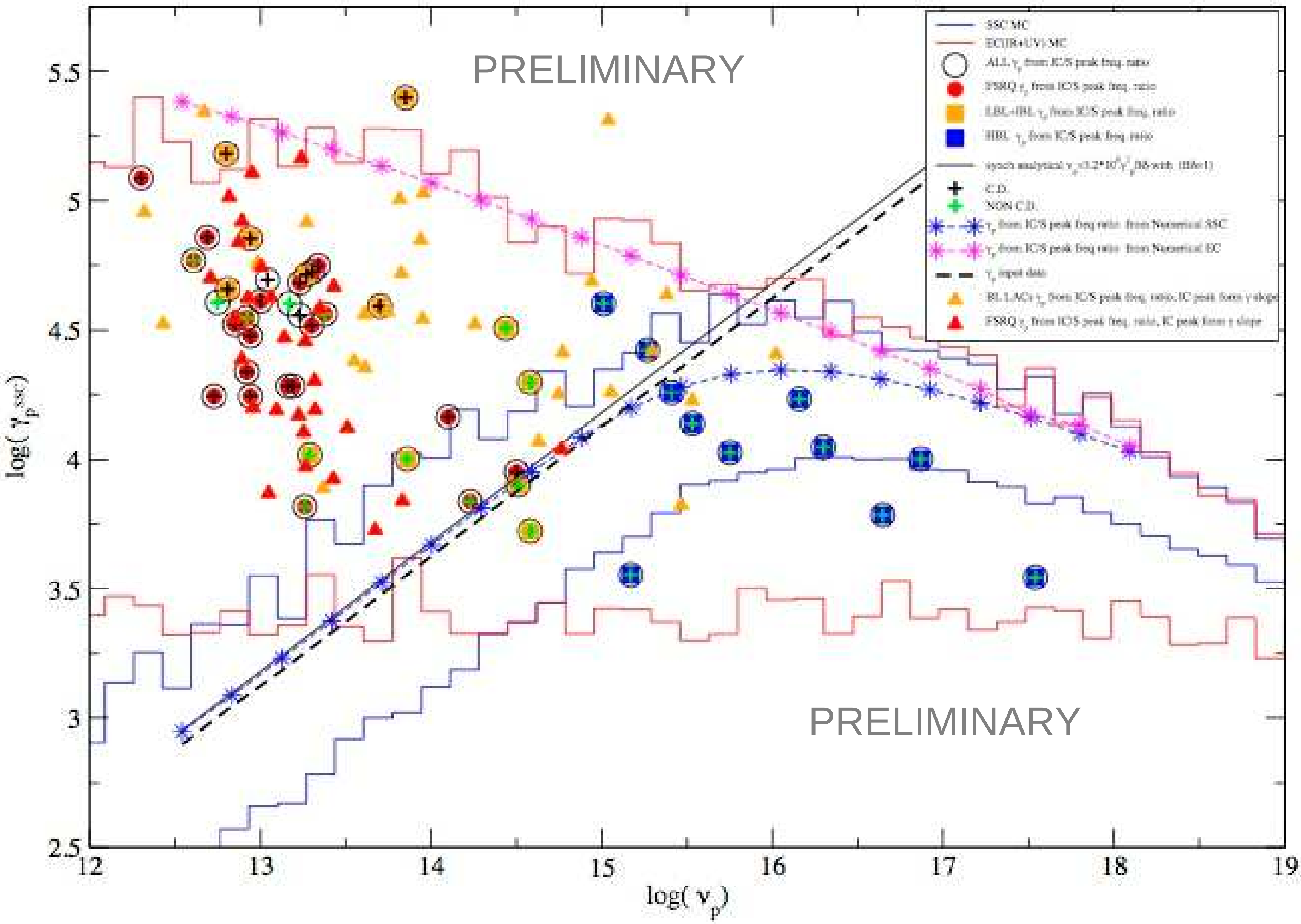
PRELIMINARY
PRELIMINARY
SSC MC
EC(IR+UV) MC
C.D.
NON C.D.
log($\gamma_{p,SSC}$)
log(ν_p)
5.5
5
4.5
4
3.5
3
2.5
12
13
14
15
16
17
18
19

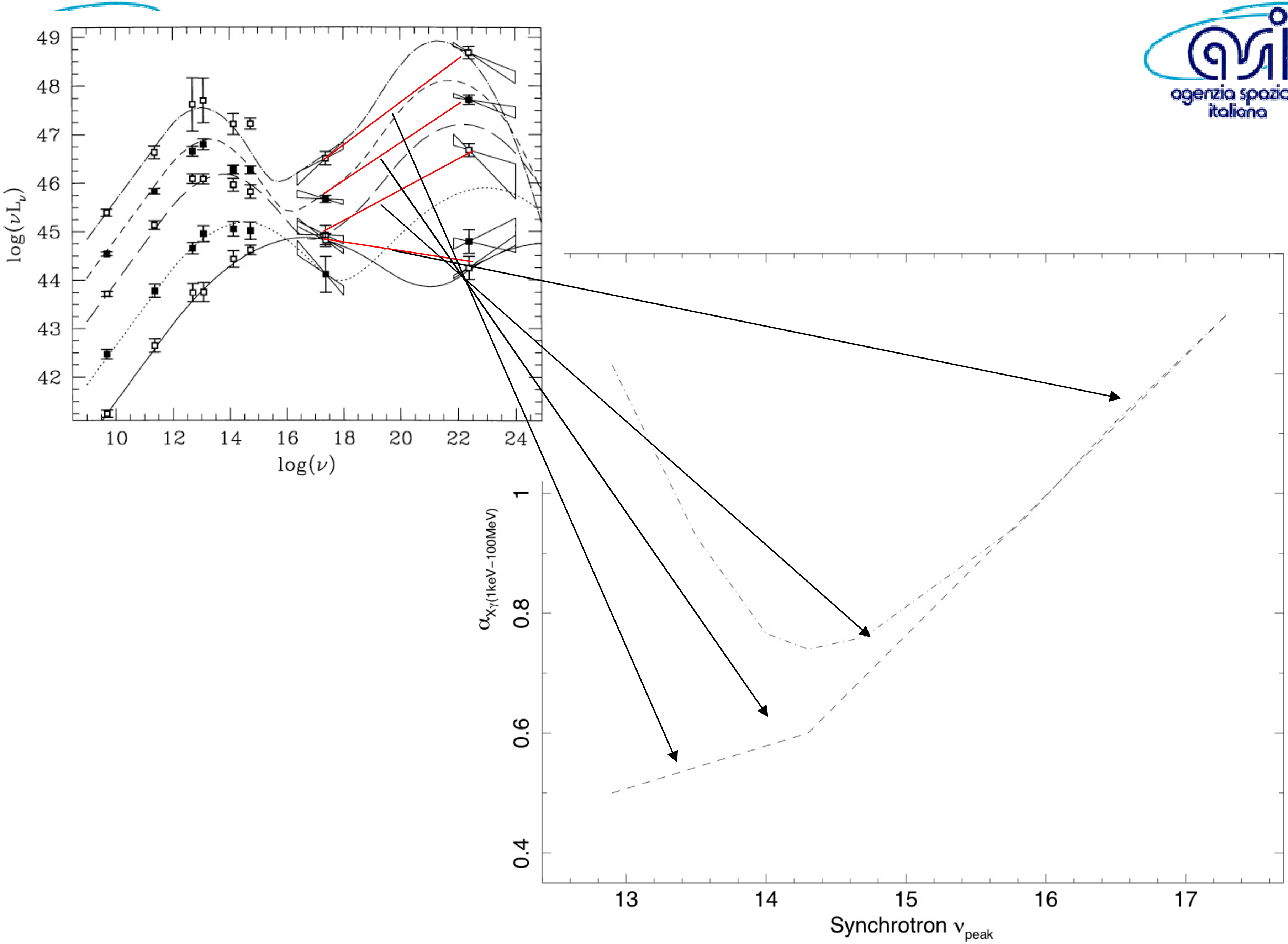

log(νL_ν)
log(ν)
49
48
47
46
45
44
43
42
10
12
14
16
18
20
22
24
α_Xγ(1keV−100MeV)
0.4
0.6
0.8
1
13
14
15
16
17
Synchrotron ν_peak

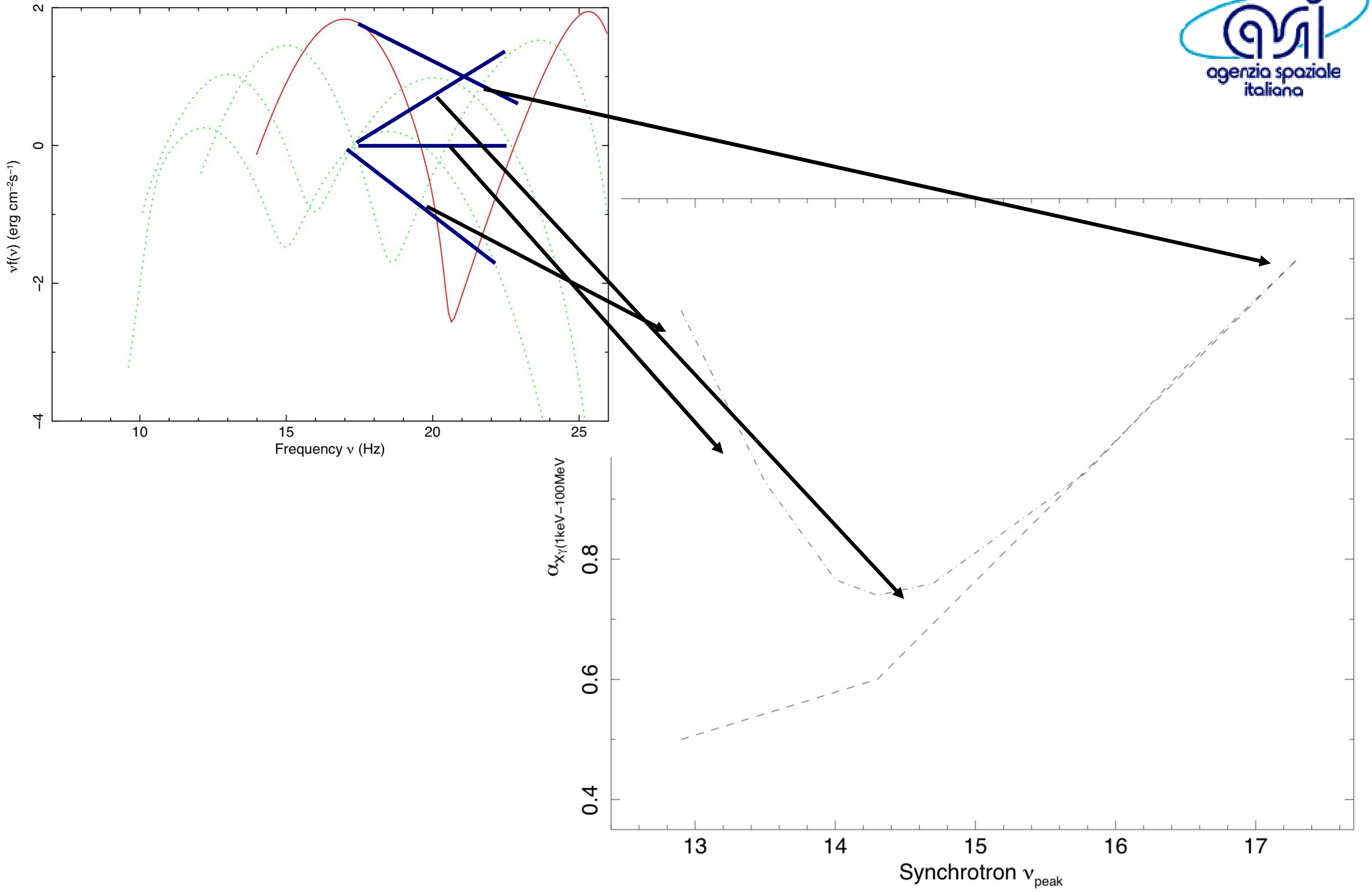
νf(ν) (erg cm−2s−1)
2
0
−2
−4
10
15
20
25
Frequency ν (Hz)
αXγ(1keV−100MeV)
0.4
0.6
0.8
13
14
15
16
17
Synchrotron νpeak

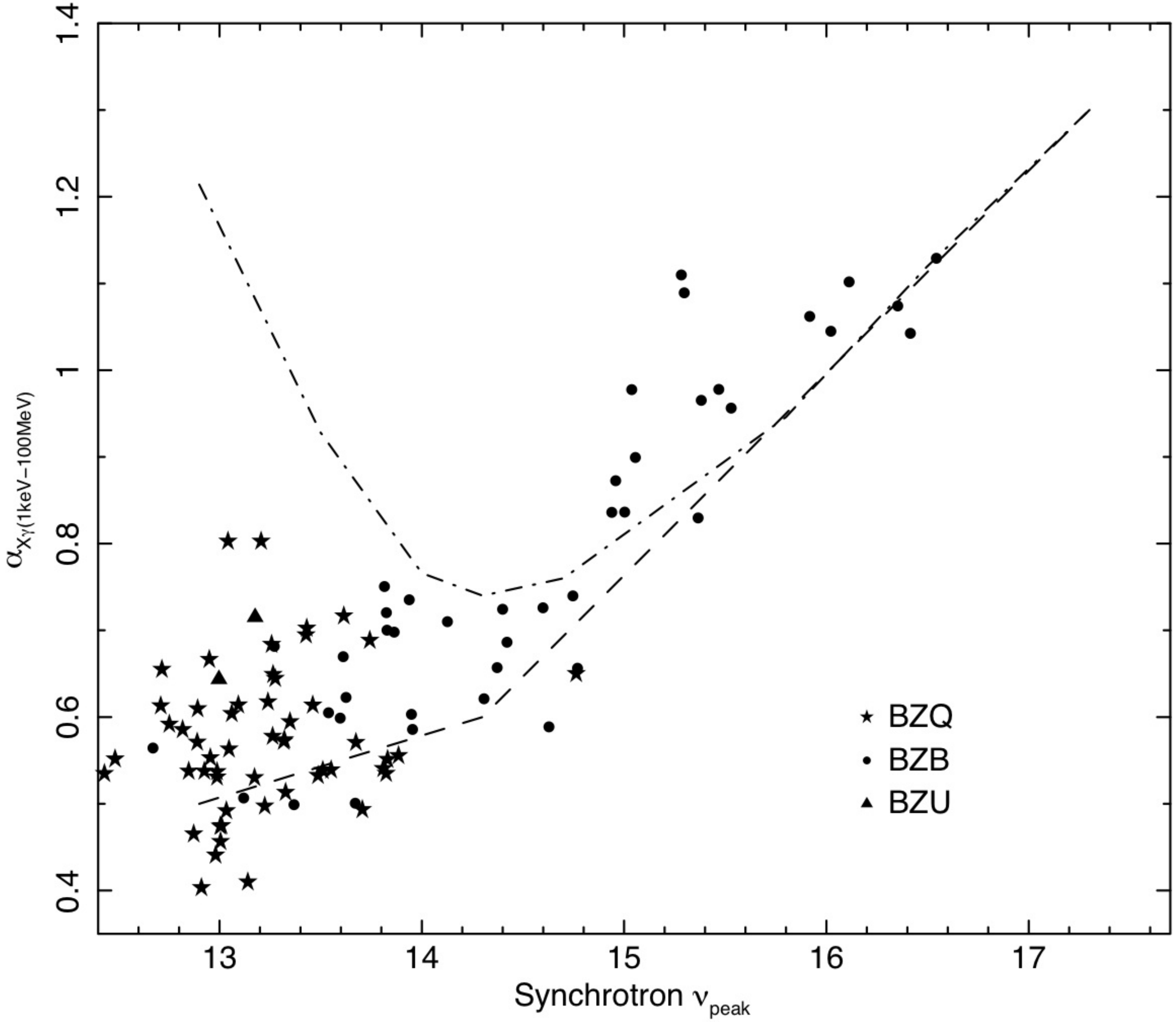
1.4
1.2
1
0.8
0.6
0.4
13
14
15
16
17
Synchrotron ν_{peak}
$\alpha_{X\gamma(1keV-100MeV)}$
BZQ
BZB
BZU

Blazar γ-ray flux upper limits

$\alpha_{ox} + \alpha_{ro} \ -> \ \nu_{peak}$

+

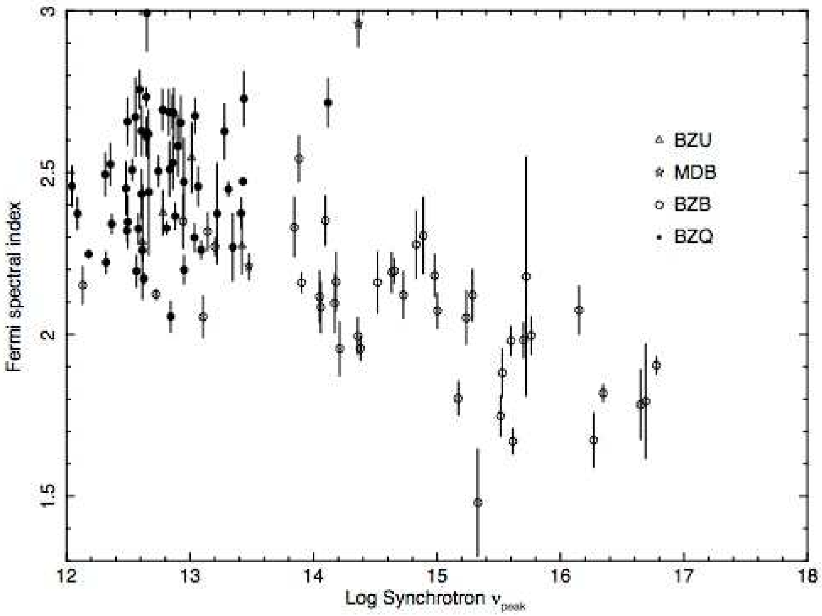

+

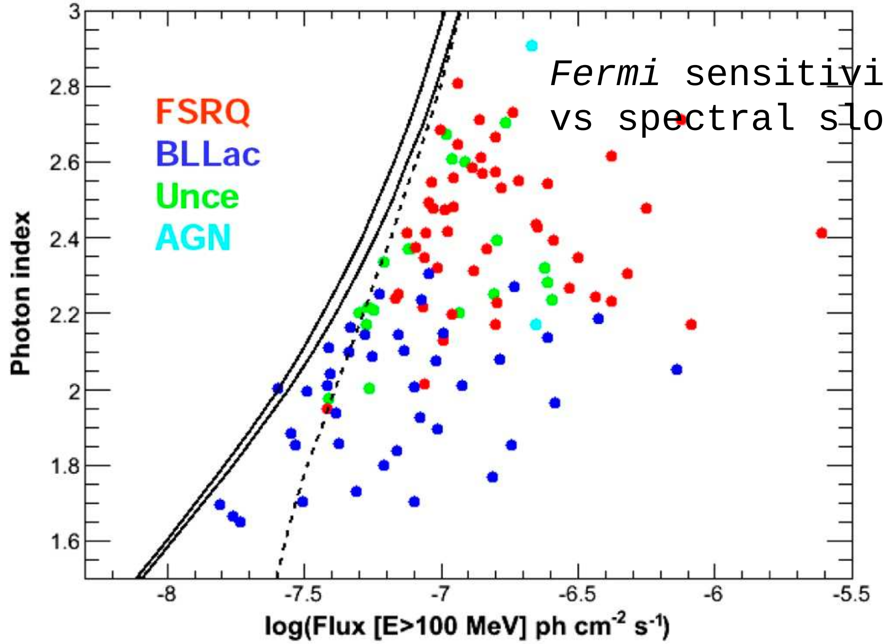

Fermi upper limits to

γ-ray flux

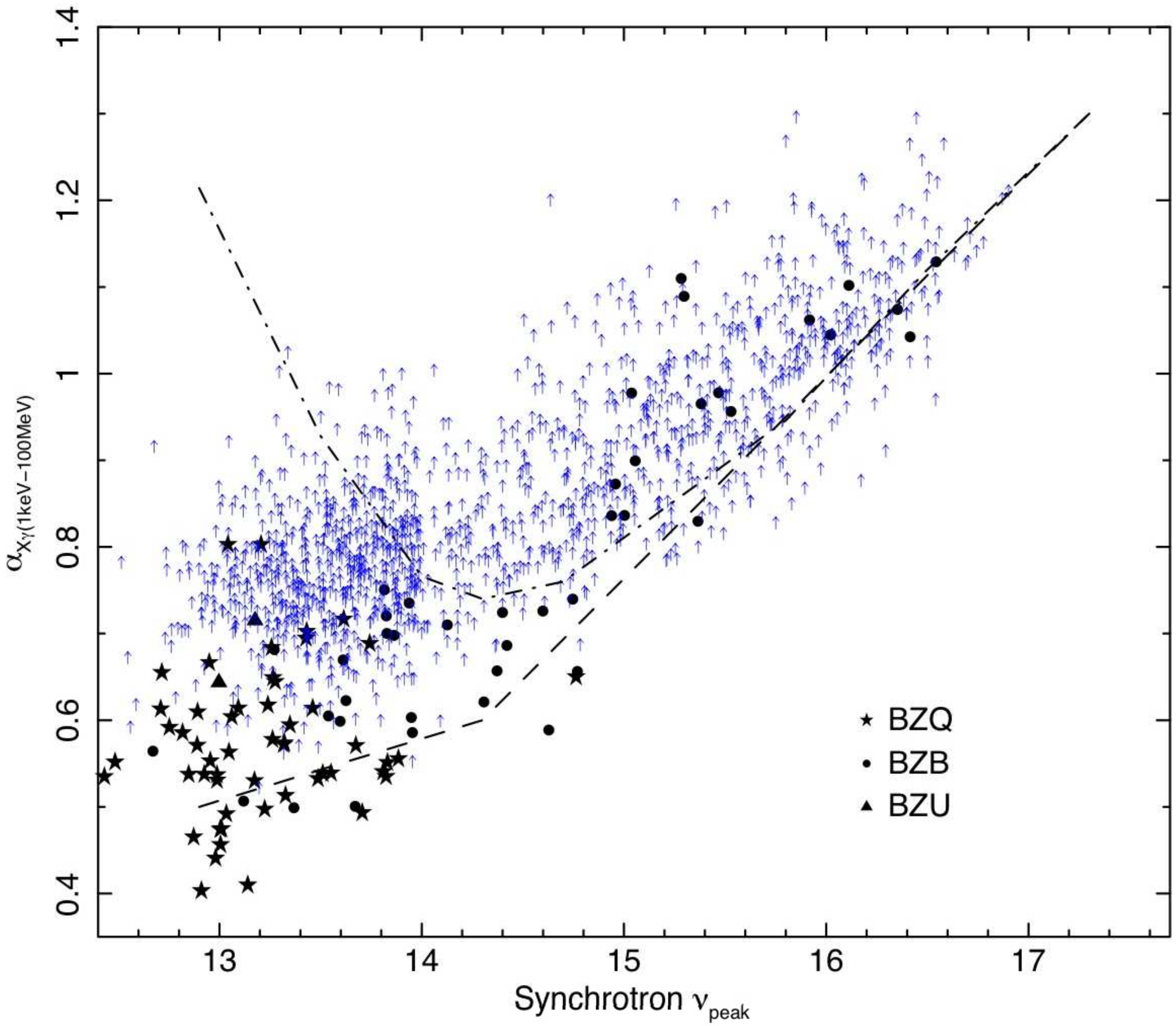
1.4
1.2
1
0.8
0.6
0.4
$\alpha_{X\gamma(1keV-100MeV)}$
13
14
15
16
17
Synchrotron ν_{peak}
BZQ
BZB
BZU

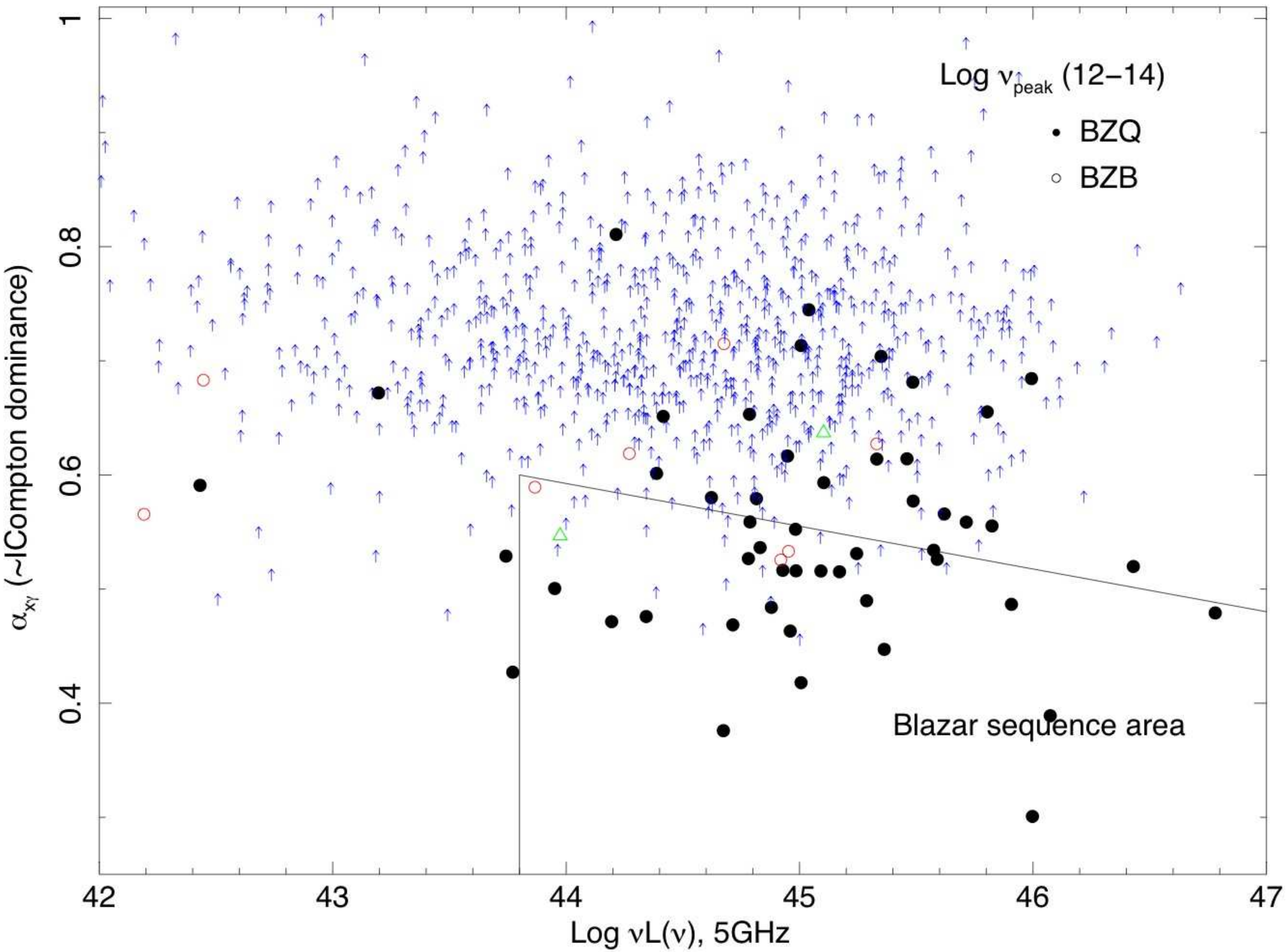
Log ν_peak (12–14)
BZQ
BZB
Blazar sequence area
α_xγ (~ICompton dominance)
Log νL(ν), 5GHz
1
0.8
0.6
0.4
42
43
44
45
46
47

Conclusions-1

- We have assembled high-quality quasi-simultaneous SED of 48 LBAS blazars. This subset is representative of the entire LBAS
- All Fermi bright blazars have broad-band spectral properties similar to radio and X-ray selected blazars (double bump SEDs, same area of aox-aro plane, no UHBLs… so far)
- We have estimated the syncrhotron and “iC” peak energy and intensities for all 106 sources in the sample.
- The distribution of synchrotron and “i-Compton” ν_{peak} distributions are very different for FSRQs and BL Lacs.

  FSRQs ν^{S}_{peak} values range between $10^{12.5}$ Hz and $10^{14.5}$ Hz

  BL Lacs ν^{S}_{peak} values range between 10^{13} Hz and 10^{17} Hz
- There is a strong correlation between both ν^{S}_{peak}, ν^{iC}_{peak} and the gamma-ray spectral slope
- The overabundance of HBL BL Lac is a selection effect similar to what experienced in the X-ray band

Conclusions-2

- HBL BL Lacs radiate close to the predictions of simple one-zone SSC models
- Over 60% of known HBL BL Lacs (f_r > 300 mJy) are detected as bright Fermi sources.
- LBAS FSRQs (and LBL BL Lacs) emit much more gamma-rays than predicted by SSC, requiring additional mechanism (e.g. EC, or multiple components)
- However, only ~13% of FSRQs (LBLs) brighter than 500 mJY in the Bzcat or in WMAP-5yr catalogs are detected in LBAS, despite having similar properties (same redshift, Vmag, ν^{S}_{peak} distributions etc). It is therefore possible/probable that the majority of FSRQs (and LBL BL Lacs) actually radiate not too far from simple SSC.